Bulletin of Mathematical Biology (2008) 70: 820–867
DOI 10.1007/s11538-007-9281-2

ORIGINAL ARTICLE

Quantifying the Routes of Transmission for Pandemic Influenza

Michael P. Atkinson[a], Lawrence M. Wein[b,*]

[a] *Institute for Computational and Mathematical Engineering, Stanford University, Stanford, CA 94305, USA*
[b] *Graduate School of Business, Stanford University, 518 Memorial Way, Stanford, CA 94305, USA*

Received: 2 January 2007 / Accepted: 3 October 2007 / Published online: 16 February 2008

Abstract Motivated by the desire to assess nonpharmaceutical interventions for pandemic influenza, we seek in this study to quantify the routes of transmission for this disease. We construct a mathematical model of aerosol (i.e., droplet-nuclei) and contact transmission of influenza within a household containing one infected. An analysis of this model in conjunction with influenza and rhinovirus data suggests that aerosol transmission is far more dominant than contact transmission for influenza. We also consider a separate model of a close expiratory event, and find that a close cough is unlikely ($\approx$1% probability) to generate traditional droplet transmission (i.e., direct deposition on the mucous membranes), although a close, unprotected and horizontally-directed sneeze is potent enough to cause droplet transmission. There are insufficient data on the frequency of close expiratory events to assess the relative importance of aerosol transmission and droplet transmission, and it is prudent to leave open the possibility that droplet transmission is important until proven otherwise. However, the rarity of close, unprotected and horizontally-directed sneezes—coupled with the evidence of significant aerosol and contact transmission for rhinovirus and our comparison of hazard rates for rhinovirus and influenza—leads us to suspect that aerosol transmission is the dominant mode of transmission for influenza.

Keywords Aerosol physics · Dose-response models · Disease transmission

1. Introduction

Pandemic influenza (influenza A subtype H5N1) is widely perceived to be one of the world's most serious near-term public health threats (Health and Human Services Department, 2004). If a strain similar in effect to the 1918 pandemic influenza emerges

*Corresponding author.
E-mail addresses: mpa33@stanford.edu (Michael P. Atkinson), wein_lawrence@stanford.edu (Lawrence M. Wein).

within the next several years, it is highly likely that an effective vaccine will not be available during the pandemic's first wave (Health and Human Services Department, 2004); the antiviral drug supply will be insufficient for large-scale prophylactic use (Homeland Security Council, 2006) and possibly ineffective (de Jong et al., 2005; Le et al., 2005), and hospitals will be too overwhelmed to treat most cases. Consequently, as in 1918, we will need to rely on voluntary and forced social distancing measures to mitigate the spread of disease, including the closing of schools and churches, the elimination of public gatherings, high worker absenteeism, and the wearing of masks in public (Markel et al., 2006).

Our research goal is to assess infection control measures in the home. However, a prerequisite for assessing infection control measures is the quantification of how much influenza transmission is due to the various routes. Much of the literature (Health and Human Services Department, 2004; Committee on the Development of Reusable Facemasks, 2006; Bridges et al., 2003; Tellier, 2006) considers three modes of transmission: droplet transmission (virus particles from an infected's sneeze or cough deposits directly onto a susceptible's mucous membranes), contact transmission (an infected gets virus on his hands and transfers this virus either directly, e.g., via a handshake, or indirectly via fomites, to the hands of a susceptible, who then places his hand into his mouth, nose or eyes) and aerosol transmission, in which a susceptible inhales droplet nuclei (i.e., evaporated virus-containing particles in the air). The relative importance of these transmission routes is unknown (Health and Human Services Department, 2004; Committee on the Development of Reusable Facemasks, 2006) and the subject of some debate (Bridges et al., 2003; Tellier, 2006).

We address these issues in a pair of studies. In the present study, we quantify the routes of transmission for influenza by formulating a detailed mathematical model of the viral shedding and transmission within a four-member household containing one infected, and using data from the literature to calibrate the model. In the companion paper (Wein and Atkinson, 2006), we embed the four-person household model from the present paper into an epidemic household model (Ball and Neal, 2002) in which between-household global contacts occur in addition to the within-household local contacts, and then assess various infection control measures, such as face protection, ventilation and humidifiers.

Because there are insufficient data to estimate the frequency of close expiratory events that could cause droplet transmission, we perform two separate analyses in this paper. In Section 2, we formulate the four-person household model, which incorporates aerosol and contact transmission, but not droplet transmission. Parameter estimation for this model is undertaken in Section 3, which allows us to compare these two routes of transmission. In Section 4, we model an isolated close expiratory event, and (inspired by Nicas and Sun, 2006) consider the three possible modes of transmission: inhalation of droplet nuclei (i.e., <10 μm particles) from the cough or sneeze, inhalation of inspirable particles in the $[10, 100]$ μm range and direct deposition onto the mucous membranes (i.e., traditional droplet transmission).

The parameter estimation procedure in Section 3 is lengthy and at times tedious; an overview of this procedure is provided at the beginning of Section 3. Briefly, existing data allow us to estimate all of the model's parameters in Section 3.1, except for a composite parameter (it is the product of four primitive parameters) that dictates the amount of contact transmission during the presymptomatic period. We indirectly estimate the value of this influenza contact transmission parameter using rhi-

novirus data. More specifically, because there exist ample data from rhinovirus transmission experiments and because many of the model's parameters are identical for interpandemic influenza and rhinovirus (including the mixing behavior during the presymptomatic period and some physiological and environmental parameters), we recalibrate the model with rhinovirus data in Section 3.2 and perform a cross-disease comparison in Section 3.3. Readers interested in only the essence of our argument may want to focus on Section 3.3, where we develop mathematical expressions for the hazard rates associated with aerosol transmission and contact transmission in a somewhat simplified setting, and compute the influenza-to-rhinovirus hazard rate ratio for these two transmission modes with the aid of the data in Table 2. The values of these ratios, combined with a reanalysis of some rhinovirus experiments (Meschievitz et al., 1984; Dick et al., 1987) in Appendices A and B, and an upper-bounding procedure in Section 3.4, allow us to estimate the presymptomatic contact transmission parameter. Substituting all of the influenza parameter values into the detailed household model from Section 2, which we do for interpandemic influenza and pandemic influenza in Section 3.5 and Section 3.6, allows us to conclude that the contribution from contact transmission in influenza is trivial.

After submitting this paper for publication, a closely-related paper by Nicas and Sun (2006) appeared, which to our knowledge is the first to mathematically model the multiple-pathway framework in Fig. 1a and to analyze a close expiratory event in detail. In the Discussion in Section 5, we compare our study and (Nicas and Sun, 2006), and describe how we revised our model as a result of reading (Nicas and Sun, 2006).

2. The model

This section describes the mathematical model of disease spread within a household that contains a single infected person and $n-1$ susceptibles; Fig. 1a provides a graphical depiction of the model; although Fig. 1a includes droplet transmission, this mode of transmission is deferred until Section 4. The viral dynamics are modeled in Section 2.1; the doses are calculated in Section 2.2 and the dose-response model is formulated in Section 2.3.

2.1. The viral dynamics

The infected person becomes infectious at time 0, develops symptoms at time T_p and stops being infectious at time T_I, and so we explicitly include an incubation period where the infected is infectious but does not yet have symptoms (Health and Human Services Department, 2004). This subsection develops an ordinary differential equation model for the time period $[0, T_I]$. We assume the house consists of three compartments (Fig. 1b): the living quarters (indexed by $j = 1$), the infected's bedroom ($j = 2$) and a susceptible's bedroom ($j = 3$). We do not explicitly model multiple susceptible bedrooms, and hence ignore the small amount of virus that could leak out of the living quarters and into these other bedrooms. There are seven state variables: the concentration of virus in particles of diameter x in the air at time t in each of the three compartments ($C_{aj}(x, t)$ for $j = 1, 2, 3$), the concentration of virus on porous surfaces at time t in compartments 1 and 2 ($C_{p1}(t)$, $C_{p2}(t)$) and the concentration of virus on nonporous surfaces at time t in compartments

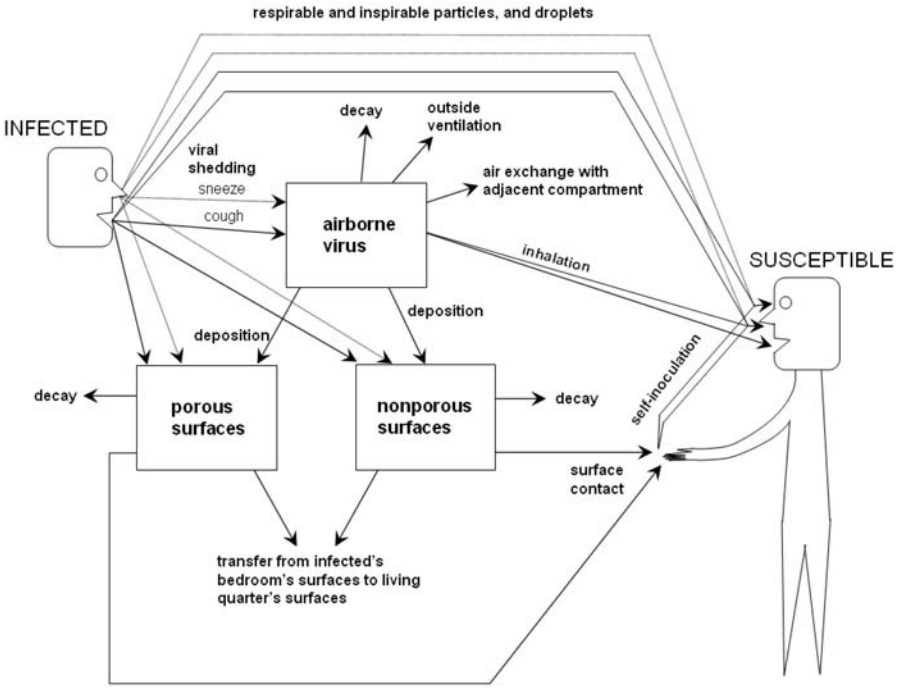

(a)

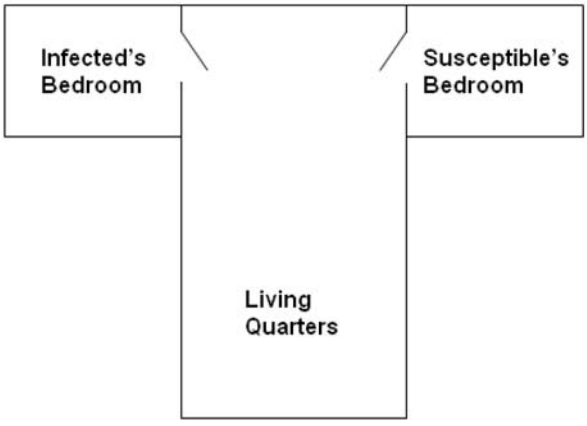

(b)

Fig. 1 (a) A graphical depiction of the model. (b) The three-compartment household.

1 and 2 ($C_{n1}(t)$, $C_{n2}(t)$). We distinguish between porous and nonporous surfaces because the death rate of the virus is significantly different between the two surfaces. Also, the particle diameters reported in this study pertain to when the particles are in the airways of

either the susceptible or infected. In the ambient air, particle diameters shrink by a factor of 2 (Nicas et al., 2005).

There are several differences in the model between the presymptomatic phase $[0, T_p]$ and the symptomatic phase $(T_p, T_I]$. The infected person stays in his bedroom throughout the symptomatic period and one of the susceptibles, referred to as the caregiver, spends some time in the infected bedroom to provide care; during the symptomatic period, the other $n-2$ noncaregiving susceptibles never go into the infected's bedroom. In addition, as described in Section 3, some of the parameters take on different values in the presymptomatic and symptomatic periods to reflect increased social distancing.

We use the indicator functions $I_{ij}(t)$ to describe the presence or absence of person i ($i=1$ for infected, $i=2$ for noncaregiving susceptible, $i=3$ for caregiver) in compartment j. During the presymptomatic period, each person spends Δ_1 hours each day in the living quarters followed by Δ_2 hours in his bedroom, and is out of the house for $24-\Delta_1-\Delta_2$ hours. We assume that these times are perfectly synchronized, so that each family member is in his bedroom, in the living quarters or out of the house during the same hours. The noncaregiving symptomatics follow this same schedule throughout the symptomatic period, and the caregiver does also, except for spending Δ_3 hours providing care in the infected's bedroom in lieu of being out of the house. The indicator functions (where time is in hours and τ_1 and τ_3 specify the beginning of the living quarters time and the caregiving time, respectively, and where $x^+ = \max\{x, 0\}$—note also that $T_p = 24$ hr) are

$$I_{11}(t) = \begin{cases} 1 & \text{for } t \in [(24i+\tau_1)^+, \min\{(24i+\tau_1+\Delta_1)^+, T_p\}) \\ & \quad \text{for } i = -1, \ldots, \frac{T_p}{24} - 1, \\ 0 & \text{otherwise,} \end{cases} \tag{1}$$

$$I_{12}(t) = \begin{cases} 1 & \text{for } t \in [\min\{(24i+\tau_1+\Delta_1)^+, T_p\}, \\ & \qquad \min\{(24i+\tau_1+\Delta_1+\Delta_2)^+, T_p\}) \cup t \in [T_P, T_I] \\ & \quad \text{for } i = -1, \ldots, \frac{T_p}{24} - 1, \\ 0 & \text{otherwise,} \end{cases} \tag{2}$$

$$I_{21}(t) = \begin{cases} 1 & \text{for } t \in [(24i+\tau_1)^+, \min\{(24i+\tau_1+\Delta_1)^+, T_I\}) \\ & \quad \text{for } i = -1, \ldots, \frac{T_I}{24} - 1, \\ 0 & \text{otherwise,} \end{cases} \tag{3}$$

$$I_{31}(t) = \begin{cases} 1 & \text{for } t \in [(24i+\tau_1)^+, \min\{(24i+\tau_1+\Delta_1)^+, T_I\}) \\ & \quad \text{for } i = -1, \ldots, \frac{T_I}{24} - 1, \\ 0 & \text{if } I_{32}(t) = 1, \\ 0 & \text{otherwise,} \end{cases} \tag{4}$$

$$I_{23}(t) = \begin{cases} 1 & \text{for } t \in [\min\{(24i+\tau_1+\Delta_1)^+, T_I\}, \\ & \qquad \min\{(24i+\tau_1+\Delta_1+\Delta_2)^+, T_I\}) \\ & \quad \text{for } i = -1, \ldots, \frac{T_I}{24} - 1, \\ 0 & \text{otherwise,} \end{cases} \tag{5}$$

$$I_{33}(t) = \begin{cases} 1 & \text{for } t \in [\min\{(24i + \tau_1 + \Delta_1)^+, T_I\}, \\ & \qquad \min\{(24i + \tau_1 + \Delta_1 + \Delta_2)^+, T_I\}) \\ & \quad \text{for } i = -1, \ldots, \frac{T_I}{24} - 1, \\ 0 & \text{if } I_{32}(t) = 1, \\ 0 & \text{otherwise,} \end{cases} \tag{6}$$

$$I_{32}(t) = \begin{cases} 1 & \text{for } t \in [24i + \tau_3, 24i + \tau_3 + \Delta_3) \quad \text{for } i = 1, \ldots, \frac{T_I}{24} - 1, \\ 0 & \text{otherwise,} \end{cases} \tag{7}$$

and $I_{13}(t) = I_{22}(t) = 0$ for $t \in [0, T_I]$. In the base case, we assume that bedroom doors are closed when the bedroom is occupied and open when the bedroom is unoccupied.

Let $\lambda(t)$ be the rate of viral shedding at time $t \in [0, T_I]$. We assume that the viral shedding rate grows exponentially at rate ν starting from the level Λ_0 during the presymptomatic phase and then drops exponentially at rate ω during the symptomatic phase, so that

$$\lambda(t) = \begin{cases} \Lambda_0 e^{\nu t} & \text{for } t \in [0, T_p], \\ \Lambda_0 e^{\nu T_p - \omega(t - T_p)} & \text{for } t \in [T_p, T_I]. \end{cases} \tag{8}$$

Equation (8) is consistent with the observation that viral shedding is maximal at the time when symptoms appear, and decreases exponentially thereafter (Douglas, 1975; Hall et al., 1979). To capture the interperson heterogeneity in viral shedding, we let Λ_0 be a log-normal random variable with probability density function $h(\lambda)$, where the natural logarithm of the initial shedding rate has mean m_λ (i.e., the median initial shedding rate is e^{m_λ}) and standard deviation σ_λ (i.e., the dispersion is e^{σ_λ}). Although it may make more physical sense to let the initial shedding rate Λ_0 be a fixed small number and let the rate ν be random in Eq. (8) rather than vice-versa, transmission is dominated by the peak shedding rate (as we show later) and our results are very insensitive to the initial shedding rate. Hence, both approaches (i.e., Λ_0 random or ν random) give similar results.

Compartment j has air volume V_j, surface area A_j and ventilation (i.e., outdoor air supply) rate Q_j. In addition, Q_{ij} is the air flow rate from compartment i to compartment j, where $Q_{23} = Q_{32} = 0$. We assume that all particles immediately shrink to half of their original size after emission from an infected. Particles smaller than d_c in diameter immediately evaporate in the air and become droplet nuclei, and all particles with diameter larger than d_c instantaneously settle on a surface within several meters of the infected person; the actual times until evaporation for sub-d_c particles and settling times for super-d_c particles are orders-of-magnitude smaller than T_p (Nicas et al., 2005; Wells, 1955). In this part of the model, we ignore inhalation of particles larger than d_c, which could occur if an infected coughs or sneezes directly in front of a susceptible and the susceptible takes an immediate breath, inhaling the larger particles before they settle on the surfaces; we investigate this type of transmission in Section 4.2. Let $p(x)$ be the probability density function (pdf) of particle sizes (i.e., diameters) emitted by the infected (before evaporation), which represents a weighted average of particle sizes emitted during coughing and sneezing. Because the amount of virus in a particle is roughly proportional to the particle's volume (Couch et al., 1965), we define $f(x) = \frac{x^3 p(x)}{\int_0^\infty x^3 p(x)\,dx}$, which is the pdf for the proportion of shed virus that is in particles of each size, and let $\bar{F}(x)$ denote

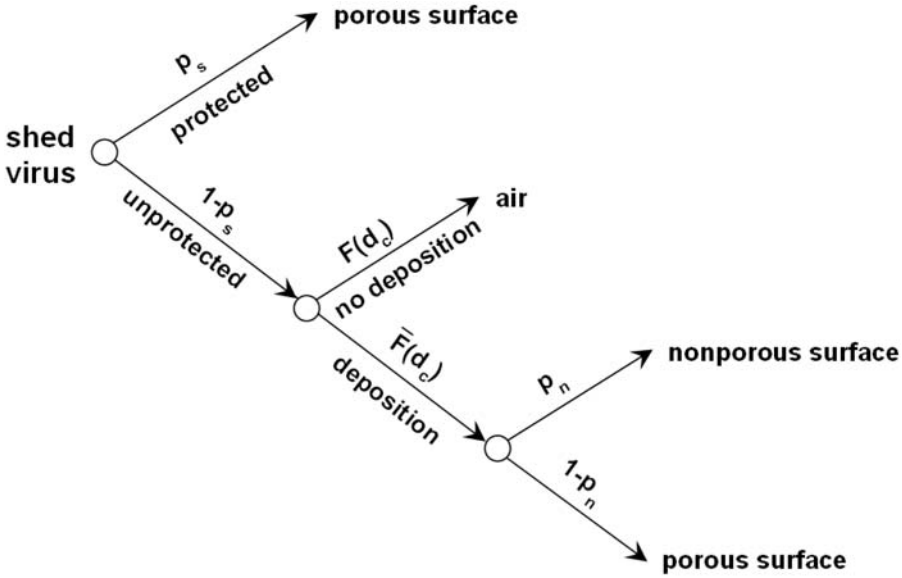

Fig. 2 The fraction of shed virus that deposits in the air and on porous and nonporous surfaces.

the complementary cumulative distribution function. The death rate of virus is μ_a in the air, μ_p on the porous surfaces, μ_n on the nonporous surfaces, and μ_h on the hands. By Stokes law, we assume that an airborne particle of diameter x settles on the surfaces at a rate proportional to the diameter squared (Heinsohn and Cimbala, 1999), which we denote by κx^2. Thus, the total settling rate at time t of the virus concentration from the air to surfaces in compartment j is given by $\int_0^{d_c} C_{aj}(x,t)\kappa x^2\,dx$. As shown in Fig. 2, we also assume that at each point in time and independent of particle size, a fraction p_s of the shed virus ends up on porous surfaces due to protective measures on the part of the infected (e.g., the virus lands on tissues for a sneeze, or hands for a cough). Of the remaining fraction of particles that is not airborne (i.e., $((1-p_s)\bar{F}(d_c))$, a fraction p_{nj} settles on nonporous surfaces and a fraction $1-p_{nj}$ settles on porous surfaces in compartments $j=1,2$. In compartment j, we assume that the shed virus settles on surfaces in an area a_j that is smaller than the total compartment surface area A_j. The particles that settle on the surfaces from the air compartment also settle on porous and nonporous surfaces according to the fractions $1-p_{nj}$ and p_{nj}. We ignore the possibility of a susceptible getting infected in his bedroom from contact with surfaces that are contaminated by virus settling from the air.

Finally, leakage of surface virus from the infected bedroom, which is caused by the movement of contaminated items, occurs at rate δ while the infected is in his bedroom during the presymptomatic period and while the caregiver is in the infected's bedroom during the symptomatic period. A fraction p_{n2} of the transferred contaminated items is nonporous and a fraction $1-p_{n2}$ is porous. A fraction p_d of the leaked surface virus on these transferred items is disposed of, while the remainder ends up as surface virus in the living quarters. If we let $I_{\{x\}}$ denote the indicator function of the event x, then the above

description implies that

$$\dot{C}_{a1}(x,t) = \frac{f(x)(1-p_s)\lambda(t)I_{11}(t)}{V_1} + \frac{Q_{21}C_{a2}(x,t) + Q_{31}C_{a3}(x,t)}{V_1} - \left[\frac{Q_1+Q_{12}+Q_{13}}{V_1} + \mu_a + \kappa x^2\right]C_{a1}(x,t) \quad \text{for } x \in [0,d_c], \tag{9}$$

$$\dot{C}_{p1}(t) = \frac{[p_s + (1-p_s)(1-p_{n1})\bar{F}(d_c)]\lambda(t)I_{11}(t)}{a_1} + \frac{(1-p_{n1})V_1}{A_1}\int_0^{d_c} C_{a1}(x,t)\kappa x^2\,dx + \delta\left[I_{12}(t)I_{\{t\le T_P\}} + I_{32}(t)\right](1-p_d)(1-p_{n2})C_{p2}(t) - \mu_p C_{p1}(t), \tag{10}$$

$$\dot{C}_{n1}(t) = \frac{(1-p_s)p_{n1}\bar{F}(d_c)\lambda(t)I_{11}(t)}{a_1} + \frac{p_{n1}V_1}{A_1}\int_0^{d_c} C_{a1}(x,t)\kappa x^2\,dx + \delta\left[I_{12}(t)I_{\{t\le T_P\}} + I_{32}(t)\right](1-p_d)p_{n2}C_{n2}(t) - \mu_n C_{n1}(t), \tag{11}$$

$$\dot{C}_{a2}(x,t) = \frac{f(x)(1-p_s)\lambda(t)I_{12}(t)}{V_2} + \frac{Q_{12}C_{a1}(x,t)}{V_2} - \left[\frac{Q_2+Q_{21}}{V_2} + \mu_a + \kappa x^2\right]C_{a2}(x,t) \quad \text{for } x \in [0,d_c], \tag{12}$$

$$\dot{C}_{p2}(t) = \frac{[p_s + (1-p_s)(1-p_{n2})\bar{F}(d_c)]\lambda(t)I_{12}(t)}{a_2} + \frac{(1-p_{n2})V_2}{A_2}\int_0^{d_c} C_{a2}(x,t)\kappa x^2\,dx - \delta\left[I_{12}(t)I_{\{t\le T_P\}} + I_{32}(t)\right](1-p_{n2})C_{p2}(t) - \mu_p C_{p2}(t), \tag{13}$$

$$\dot{C}_{n2}(t) = \frac{(1-p_s)p_{n2}\bar{F}(d_c)\lambda(t)I_{12}(t)}{a_2} + \frac{p_{n2}V_2}{A_2}\int_0^{d_c} C_{a2}(x,t)\kappa x^2\,dx - \delta\left[I_{12}(t)I_{\{t\le T_P\}} + I_{32}(t)\right]p_{n2}C_{n2}(t) - \mu_n C_{n2}(t), \tag{14}$$

$$\dot{C}_{a3}(x,t) = \frac{Q_{13}C_{a1}(x,t)}{V_3} - \left[\frac{Q_3+Q_{31}}{V_3} + \mu_a + \kappa x^2\right]C_{a3}(x,t) \quad \text{for } x \in [0,d_c]. \tag{15}$$

2.2. *The doses*

We allow two avenues for infection: aerosol transmission, in which a susceptible inhales droplet nuclei that contain virus, and contact transmission, in which an infected discharges virus onto surfaces (including the infected's hands) and a susceptible gets this virus on his hands and self-inoculates. For rhinovirus, the ID_{50} in the mouth is 8,000-fold higher than the ID_{50} in the nose (D'Alessio et al., 1984), and the ID_{50}s in the nose and eyes are comparable because the virus does not infect the eyes but appears to travel from the

eyes to the nasal mucosa via the tear duct (Bynoe et al., 1961; Winther et al., 1986). For lack of data on the influenza ID_{50} in the mouth and eyes, we assume the same holds for influenza and that contact transmission and droplet transmission occur in the nose or eyes, but not the mouth. In the remainder of this subsection, we compute the doses received by a susceptible from both routes. The relationship between these doses and the likelihood of infection is described in Section 2.3.

If b is the breathing rate, then the total dose inhaled from particles of size x by a noncaregiving susceptible ($i = 2$) and the caregiver ($i = 3$) is

$$D_{ai}(x) = b \int_0^{T_I} \sum_{j=1}^{3} C_{aj}(x,t) I_{ij}(t)\, dt. \tag{16}$$

Turning to contact transmission, we assume that each susceptible has contacts with surfaces every γ_1^{-1} time units while in the living quarters. In addition, the caregiver has contacts with surfaces every γ_2^{-1} time units while in the infected's bedroom. Note that we assume in (7) that the caregiver visits the infected's room once per day during the symptomatic period, whereas now we are assuming that the caregiver's visits may be more frequent and shorter; in Section 3.5, we choose the value of τ_3 so that the caregiver's 1-hr time block gives roughly the same exposure as short frequent visits throughout the day. During each contact, we assume that a fraction h_j of the porous and nonporous surface virus is transferred to the susceptible in compartment j, and hence this contact actually represents a sustained interaction with the surfaces. A susceptible washes his hands immediately after a fraction p_{hj} of contacts in a deterministic manner in compartment j, which eliminates all virus from the hands. Hence, the effective (i.e., potentially-infecting) contacts occur every $[(1 - p_{hj})\gamma_j]^{-1}$ time units. If we assume the virus death rate on hands, μ_h, is larger than the contact rate, γ_j (this would certainly be true for influenza), the virus concentration on the susceptible's hands will typically be much smaller just before a contact than just after a contact. To simplify our analysis, we assume that the virus concentration on the susceptible's hands is zero just before each new contact, so that we can analyze each effective contact in isolation. In particular, if a new contact occurs at time τ, then the virus concentration (virus is measured in units of $TCID_{50}$, which is the amount of virus that infects 50% of cells in tissue culture, and so the virus concentration is measured in $TCID_{50}/m^2$) on a susceptible's hands in compartment j is $h_j[C_{pj}(\tau) + C_{nj}(\tau)]e^{-\mu_h(t-\tau)}$ for $t \in [\tau, \tau + \gamma_j^{-1})$.

For $j = 1, 2$, susceptibles in compartment j place fingers into their nose or eyes every θ_j^{-1} time units. We assume that a fraction β of the virus on a susceptible's hands are deposited to his nose or eyes during each self-inoculation, and we let A_h denote the surface area of a susceptible's hands. For ease of presentation, we first consider the contact dose by a susceptible during the presymptomatic period, which is

$$h_1 \beta A_h \sum_{j=1}^{\lfloor \theta_1/\gamma_1 \rfloor} e^{\frac{-j\mu_h}{\theta_1}} \sum_{i=1}^{\lfloor (1-p_{h1})\gamma_1 \Delta_1 \rfloor} \left[C_{p1}\left(\tau_1 + \frac{i}{(1-p_{h1})\gamma_1}\right) + C_{n1}\left(\tau_1 + \frac{i}{(1-p_{h1})\gamma_1}\right)\right]. \tag{17}$$

The inner summation in (17) is for each specific contact a susceptible has with contaminated surfaces while in the living quarters during the presymptomatic period, whereas the outer summation is for the multiple self-inoculations that occur after each contact (adjusted for the decay of the virus on the hands). Noting that $\sum_{j=1}^{\lfloor \theta_1/\gamma_1 \rfloor} e^{-\frac{j\mu_h}{\theta_1}} = \frac{e^{-\frac{\mu_h}{\theta_1}} - e^{-\frac{\mu_h}{\theta_1}(\lfloor \theta_1/\gamma_1 \rfloor + 1)}}{1 - e^{-\frac{\mu_h}{\theta_1}}}$ and assuming $\theta_1 \gg \gamma_1$, we approximate the first sum in (17) by $\frac{e^{-\frac{\mu_h}{\theta_1}}}{1 - e^{-\frac{\mu_h}{\theta_1}}}$. Also, the second sum in (17) can be viewed as the Riemann sum $\frac{1}{n}\sum_{i=1}^{\lfloor n\Delta_1 \rfloor} f(\frac{\tau_1 + i}{n})$, where $n = (1 - p_{h1})\gamma_1$, and replacing it with the integral $\int_{\tau_1}^{\tau_1+\Delta_1} f(x)\,dx$ allows us to approximate the quantity in Eq. (17) by

$$\frac{h_1 \beta A_h (1 - p_{h1})\gamma_1 e^{-\frac{\mu_h}{\theta_1}}}{1 - e^{-\frac{\mu_h}{\theta_1}}} \int_{\tau_1}^{\tau_1+\Delta_1} \big[C_{p1}(t) + C_{n1}(t)\big]\,dt. \tag{18}$$

Using the reasoning behind Eqs. (17, 18), we approximate the total contact dose for a noncaregiving susceptible ($i = 2$) and the caregiver ($i = 3$) by

$$D_{si} = \sum_{j=1}^{2} \left(\frac{h_j \beta A_h (1 - p_{hj})\gamma_j e^{-\frac{\mu_h}{\theta_j}}}{1 - e^{-\frac{\mu_h}{\theta_j}}} \int_0^{T_I} I_{ij}(t)\big[C_{pj}(t) + C_{nj}(t)\big]\,dt \right). \tag{19}$$

2.3. The dose-response relationship

In this subsection, we derive the probability that a susceptible gets infected in terms of the doses $D_{ai}(x)$ and D_{si} in Eqs. (16) and (19). Human influenza virus preferentially binds to α2-6-linked sialic acids on receptors of ciliated columnar epithelial cells, leading to viral replication in the respiratory epithelium (Rogers and D'Souza, 1989; Connor et al., 1994). Let $g(x)$ be the fraction of inhaled particles of size x that is deposited on the respiratory epithelium. Then the total dose deposited on the respiratory epithelium for noncaregiving susceptibles ($i = 2$) and the caregiver ($i = 3$) is

$$\bar{D}_{ai} = \int_0^{d_c} D_{ai}(x) g(x)\,dx. \tag{20}$$

We use the Poisson model to compute the likelihood of infection, which is standard in the literature and which has been shown to model influenza infection and other airborne infections reasonably well (Wells, 1955; Meschievitz et al., 1984). Let ID_{50}^a denote the ID_{50} for inhaled virus deposited in the respiratory epithelium. As noted earlier, we assume that self-inoculation and droplet transmission occur via the nose or eyes, but not the mouth. Because the nose and eyes have similar ID_{50}s for rhinovirus, and for lack of data on the influenza ID_{50} in the conjunctiva for influenza, we assume that self-inoculation and droplet transmission have the same ID_{50}, which is taken to be the nasal ID_{50}, denoted by ID_{50}^n. We define the constants $\alpha_a = \frac{\ln 2}{\mathrm{ID}_{50}^a}$ and $\alpha_n = \frac{\ln 2}{\mathrm{ID}_{50}^n}$ to be used in the probability calculation.

If we write the doses in (19), (20) as functions of the initial viral shedding rate Λ_0, which has pdf $h(\lambda)$, then the probability that a noncaregiving susceptible ($i = 2$) and

the caregiver ($i = 3$) become infected, assuming probabilistic independence between the various modes of infection, is

$$P_{Ii} = 1 - \int_0^\infty e^{-(\alpha_a \bar{D}_{ai}(\lambda) + \alpha_n D_{si}(\lambda))} h(\lambda)\, d\lambda. \tag{21}$$

3. Parameter estimation

In this section, we estimate the parameter values, which are listed in Table 1 along with the references. Although our model may seem more detailed than allowed for by the strength of the data, in Section 5 we perform a sensitivity analysis on those parameters that we suspect could influence our main result about the dominance of aerosol transmission over contact transmission. All parameters are estimated in Section 3.1 except a composite parameter ϕ_1 that is the product of four contact transmission parameters. In addition, our estimate of the median shedding rate e^{m_λ} in Section 3.1 is suspect, and so we need an alternative method to estimate this parameter.

We resort to rhinovirus transmission data to estimate the composite parameter ϕ_1 for influenza. Our rationale is that the rhinovirus data are more voluminous than the influenza data, and many of the model parameters are the same for both diseases—including the mixing behavior of family members during the presymptomatic period—which facilitates cross-disease comparison; in particular, the parameter ϕ for rhinovirus should equal the presymptomatic parameter ϕ_1 for interpandemic influenza. The relative importance of each transmission mode for rhinovirus remains elusive although sustained research programs several decades ago at University of Wisconsin (Jennings and Dick, 1987) and University of Virginia (Hendley and Gwaltney, 1988) implicate the aerosol and contact routes, respectively. In Section 3.2, we estimate the rhinovirus parameter values that differ from the influenza values.

Section 3.3 contains the crux of our analysis: we derive mathematical expressions for the hazard rates (i.e., the terms in the exponent of Eq. (21)) in a somewhat simpler setting than that in Section 2, and use the parameter values from Sections 3.1 and 3.2 to numerically compute the influenza-to-rhinovirus hazard rate ratios for aerosol transmission and contact transmission. While the numerical values of these ratios are revealing, they are not sufficient to infer the relative importance of each transmission route.

At the end of Section 3.3, we are still in need of the presymptomatic composite parameter ϕ_1 for influenza and an alternative estimate for the mean shedding rate e^{m_λ} for influenza. Our first goal is to estimate ϕ_1 for influenza, which we assume is equal to the corresponding value ϕ for rhinovirus. This leads us to reanalyze several sets of rhinovirus experiments: some airborne transmission experiments (Dick et al., 1987) in Appendix A that permit us to estimate the rhinovirus mean shedding rate e^{m_λ} (this is a prerequisite for estimating the rhinovirus ϕ), and a set of rhinovirus experiments that allows all modes of transmission (Meschievitz et al., 1984) in Appendix B; these sections are relegated to the Appendix because of their tedious nature and because they are a peripheral, albeit necessary, part of our analysis.

While the reanalyses of rhinovirus data in Appendices A and B generate new insights and are suggestive of the dominant role of the aerosol mode of transmission for rhinovirus, they are far from conclusive. Moreover, these reanalyses offer no way of obtaining a

Table 1 Base-case parameters values. The subscripts 1, 2 and 3 represent the three compartments in our model. Tildes represent values during the symptomatic period. We only need to estimate the product $\phi_j = h_j \beta \gamma_j A_h$ rather than each parameter individually

Parameter	Description	Value	References
T_I	Total infectious period	120 hr	Cauchemez et al. (2004), Hayden et al. (1998)
T_p	Pre-symptomatic infectious period	24 hr	Health and Human Services Department (2004), Ferguson et al. (2005)
$\Delta_1, \Delta_2, \Delta_3$	Time Durations	8, 12, 1 hr	Section 3.1
τ_1, τ_3	Time Schedules	13, 11 hr	Sections 3.4, 3.5
ν	Pre-symptomatic viral shedding parameter	4.94/day	Hayden et al. (1998)
ω	Symptomatic viral shedding parameter	1.70/day	Hayden et al. (1998)
e^{m_λ}	Median initial viral shedding rate	2.88×10^7 TCID_{50}/day	Nicas et al. (2005), Hayden et al. (1998), Knight et al. (1970), Loudon and Brown (1967)
e^{σ_λ}	Dispersal of initial viral shedding rate	40	Meschievitz et al. (1984), Hall et al. (1979), Gwaltney et al. (1978)
V_1, V_2, V_3	Volume	228.3, 32.6, 32.6 m^3	Section 3.1
A_1, A_2, A_3	Surface area	685.0, 97.9, 97.9 m^2	Wallace (1996)
a_1, a_2	Restricted surface area	137.0, 23.0 m^2	Section 3.1
Q_1, Q_2, Q_3	Ventilation rate	228.3, 32.6, 32.6 m^3/hr	Heinsohn and Cimbala (1999)
Q_{13}, Q_{31}	Internal air flow rate (door open)	60, 60 m^3/hr	Miller and Nazaroff (2001)
Q_{12}, Q_{21}	Pre-symptomatic internal air flow rate (door open)	60, 60 m^3/hr	Miller and Nazaroff (2001)
$\tilde{Q}_{12}, \tilde{Q}_{21}$	Symptomatic internal air flow rate (door closed)	1, 1 m^3/hr	Miller and Nazaroff (2001)
d_c	Critical diameter for droplet nuclei	20 μm	Nicas et al. (2005)
$p(x)$	pdf of pre-evaporation particle diameter	Eq. (22)	Nicas et al. (2005), Loudon and Roberts (1967), Duguid (1946)
μ_a	Death rate of virus in air	0.36/hr	Hemmes et al. (1960)
μ_p	Death rate of virus on porous surfaces	1.78/hr	Bean et al. (1982)
μ_n	Death rate of virus on non-porous surfaces	0.12/hr	Bean et al. (1982)
μ_h	Death rate of virus on hands	55.3/hr	Bean et al. (1982)
κ	Settling parameter	0.18/hr μm^2	Wallace (1996), Phelps (1942)
$p_s, \tilde{p}_s$	Fraction of virus to protective surfaces	0.75, 0.5	Section 3.1
p_{n1}, p_{n2}	Fraction of virus to non-porous surfaces	0.5, 0.25	Section 3.1
δ	Fraction of surface virus transferred	0.1	Section 3.1

Table 1 (*Continued*)

Parameter	Description	Value	References
$p_d, \tilde{p}_d$	Fraction of leaked virus disposed	0.25, 0.5	Section 3.1
b	Breathing rate	20 m^3/day	Hinds (1982)
γ_1, γ_2	Surface contact rate	$\gamma_2 = 10\gamma_1$	Section 3.1
$p_{h1}, \tilde{p}_{h1}, p_{h2}$	Handwashing probability	0.05, 0.2, 0.5	Section 3.1
h_1, h_2	Hand absorption fraction from surfaces	$h_2 = 5h_1$	Section 3.1
θ_1, θ_2	Self-inoculation rate	5, 5/hr	Hendley et al. (1973)
β	Self-inoculation fraction		
A_h	Surface area of hands		
ϕ_1	$h_1\beta\gamma_1 A_h$	1×10^{-7} m^2/hr	Section 3.4
$g(x)$	Deposition fraction to respiratory epithelium	Fig. 3	ICRP (1994), Niinimaa et al. (1980)
ID_{50}^a	ID_{50} in respiratory epithelium	0.671 $TCID_{50}$	Alford et al. (1966)
ID_{50}^n	Nasal ID_{50}	500 $TCID_{50}$	Couch et al. (1971, 1974) Hayden et al. (1996)
α_a	$\ln 2/ID_{50}^a$	1.033 $TCID_{50}^{-1}$	
α_n	$\ln 2/ID_{50}^n$	1.386×10^{-3} $TCID_{50}^{-1}$	
n	Household size	4	Section 3.1

convincing nontrivial (i.e., nonzero) estimate for the value of the composite parameter ϕ for rhinovirus, and a different approach is needed.

In particular, the values of the influenza-to-rhinovirus hazard rate ratios in Section 3.3 suggest that we have several orders-of-magnitude leeway in showing that contact transmission is trivial for influenza. Hence, in Section 3.4, we derive a loose upper bound on the rhinovirus ϕ value (larger values of ϕ lead to more contact transmission) by maximizing the value of ϕ subject to liberal ranges on several other variables. In Section 3.5, we modify the model in Section 2 to the interpandemic influenza setting, and estimate the value of the final parameter, the median viral shedding rate e^{m_λ}, using interpandemic influenza data on the secondary attack rate in the home. We then confirm that very little contact transmission occurs in the interpandemic version of the model when we set the value of influenza ϕ_1 equal to the upper bound on rhinovirus ϕ in Section 3.4. Finally, returning to the pandemic influenza model in Section 2, we compute the contribution of contact transmission for pandemic influenza in Section 3.6 and find that it is negligible.

3.1. Basic parameter estimation for influenza

The infectious period is $T_I = 120$ hr (Cauchemez et al., 2004; Hayden et al., 1998), with the first of these 5 days being pre-symptomatic, so that $T_P = 24$ hr (Health and Human Services Department, 2004; Ferguson et al., 2005). We assume a situation similar to 1918, in which many schools and workplaces are closed and there is limited community interaction (Markel et al., 2006; Barry, 2004). We assume each susceptible spends 8 hr in the living quarters ($\Delta_1 = 8$ hr), 12 hr in his bedroom ($\Delta_2 = 12$ hr), and 4 hr out of the house each day, and the caregiver provides $\Delta_3 = 1$ hr of care per day to the infected during the symptomatic period.

Virus is shed from the nose and mouth, and the viral shedding rate is the product of the concentration of virus (in the nose or throat) times the rate of symptoms (sneezing or coughing). We multiply the mean nasal lavage fluid virus titers (Fig. 1 of Hayden et al., 1998) times the mean nasal discharge rates (Fig. 4 of Hayden et al., 1998) on days 1 and 2 in Hayden et al. (1998) (we take their day 1 to be our day 0) to obtain $\nu = \ln(\frac{6.7\times10^{3.7}}{3.8\times10^{1.8}}) = 4.94$/day, and on days 2 and 6 to obtain $\omega = -\frac{1}{4}\ln(\frac{1.9\times10^{1.3}}{6.7\times10^{3.7}}) = 1.70$/day. Virus titers from throat swabs also display exponential decay during the symptomatic period (Knight et al., 1970), and for lack of data we assume that viral shedding from coughing also follows the exponential parameters ν and ω derived from sneezing.

As an independent check, we also estimate the median initial shedding rate e^{m_λ} from seven more primitive parameters. We sum the shedding rates at time 0 in our model from sneezing and coughing. For sneezing, we multiply the nasal virus concentration of $7 \times 10^{1.8}$ TCID_{50}/mL (from day 1 in Fig. 1 of Hayden et al., 1998—note that throughout we obtain the viral concentration of nasal excretions by multiplying the reported concentration from nasal washes times the volume of wash used or recovered Reed, 1975) times 3.8 g/day (from day 1 in Fig. 4 of Hayden et al., 1998) and then divide by 1 g/mL (assuming that mucus, which is made up primarily of water, has the same density as water), giving 1678.6 TCID_{50}/day. The shedding rate from coughing at time 0 is the throat concentration (which is the throat concentration on day 1 in Knight et al., 1970, 10^3 TCID_{50}/mL, times $e^{-\nu}$, yielding 7.2 TCID_{50}/mL) times 15 coughs/hr for pneumonia patients (Loudon and Brown, 1967) times the volume per cough. The volume per cough is 470 droplets per cough (Loudon and Roberts, 1967) (an alternative estimate is 5,000 droplets per cough Duguid, 1946) times the mean droplet volume, which is $\frac{\pi}{6}\int_0^\infty x^3 p(x)\,dx$. Using the pdf $p(x)$ specified in (22), we find that the mean droplet volume is 5.73×10^7 μm^3 and hence the shedding rate from coughing at time 0 is 69.8 TCID_{50}/day, and $e^{m_\lambda} = 1{,}748$ TCID_{50}/day. Because of the large uncertainty when we combine these seven parameters, some of which are difficult to estimate in isolation, and because the particle studies in Loudon and Roberts (1967) and Duguid (1946) may have been performed on healthy individuals (Nicas et al., 2005), leading us to underestimate the shedding rate because infected people would be expected to have more discharge per sneeze or cough, later in this section, we essentially ignore the 1,748 value and estimate e^{m_λ} from other data.

To compute e^{σ_λ}, we assume that $\Lambda = cXY$, where the log-normal random variable X is the nasal viral concentration, the log-normal random variable Y is the rate of sneezing and coughing, and c is a proportionality constant. We set $e^{\sigma_X} = 10$, so that 95% of the nasal concentrations fall within 0.01 times the median and 100 times the median, as in the data for 43 children in Table 1 of Hall et al. (1979). For lack of influenza data, we estimate e^{σ_Y} from rhinovirus data in Table 1 of Gwaltney et al. (1978), which gives sneezing and coughing data for five individuals for each of 3 days. Using the unbiased estimator $\hat{\sigma}^2 = \frac{\sum_{i=1}^5 (\ln x_i - \hat{\mu})^2}{4}$, where $\hat{\mu} = \frac{\sum_{i=1}^5 \ln x_i}{5}$ and x_i is the mean (median) of the number of coughs over the 3 days gives $e^{\sigma_Y} = 3.9$ (5.1). If x_i is the mean number of sneezes over the 3 days (some people did not sneeze on some of the days) yields $e^{\sigma_Y} = 5.8$. We let $e^{\sigma_Y} = 5$. If we let ρ be the correlation between X and Y, then $\sigma_\lambda = \sqrt{\sigma_X^2 + \sigma_Y^2 + 2\rho\sigma_X\sigma_Y}$. Hence, $e^{\sigma_\lambda} = 16.6$ if X and Y are independent and $e^{\sigma_\lambda} = 50$ if X and Y are perfectly correlated ($\rho = 1$). There is evidence in Table 3 of Meschievitz et al. (1984) that X and Y are highly correlated for rhinovirus: for each of six experiments, the eighth column of this table represents the geometric mean of nasal concentration among a subset of 20–25 inoculated donors

that had the most severe symptoms (i.e., the most coughs and sneezes). The number in the subset for each experiment is given in the third column of this table, and it can be observed that there is a strong negative correlation between the geometric mean of the subset and the size of the subset, which is consistent with a strong positive correlation between the nasal concentration and the number of sneezes and coughs. Consequently, we set $e^{\sigma_\lambda} = 40$, which corresponds to $\rho = 0.77$.

The pdf $p(x)$ of preevaporation droplet size is similar for sneezing and coughing (Duguid, 1946). The most reliable (Nicas et al., 2005) cough data appear to be from Duguid (1946), and the pdf has been estimated as a mixture of two log-normals (Nicas et al., 2005), although these authors point out three potential shortcomings with the log-normal mixture: the left tail may be inaccurate because particles below 1 μm were not observed, the unbounded right tail gives some nonsensical implications and the aforementioned problem that the data may come from healthy individuals. We deal with the second shortcoming by truncating the distribution: if we let $f_1(x)$ denote a log-normal pdf with geometric mean 9.8 μm and geometric standard deviation 9.0 μm, and $f_2(x)$ be a log-normal pdf with geometric mean 160.0 μm and geometric standard deviation 1.7 μm, as in Nicas et al. (2005), then we set

$$p(x) = \begin{cases} \dfrac{0.71p_1(x)+0.29p_2(x)}{\int_0^{4000\ \mu\text{m}} 0.71p_1(x)+0.29p_2(x)\,dx} & \text{for } x \le 4000\ \mu\text{m}, \\ 0 & \text{for } x > 4000\ \mu\text{m}, \end{cases} \tag{22}$$

where the pdf is truncated at 4,000 μm (Nicas et al., 2005). To investigate the first shortcoming, we note that there our two studies that have detailed data on the pdf of particle size for diameters <2 μm: the ratio of <1 μm particles to 1–2 μm particles was 1.22 in Gerone et al. (1966) (summing over sneezes and coughs) and 0.89 in Papineni and Rosenthal (1997), whereas the ratio in the pdf $p(x)$ in Eq. (22) is 2.20. Hence, our pdf actually overestimates the number of submicron particles, although this has a negligible effect on our results because so little virus is contained in these submicron particles. Equation (22) implies that the particles that are smaller than d_c, and hence do not immediately fall to the ground, represent 45% of all particles and contain 10^{-6} of the shed virus (i.e., particles smaller than d_c comprise 10^{-6} of the total volume).

We assume that each bedroom has volume 12 × 12 × 8 ft = 32.6 m^3, and that the living quarters is seven times as large (by floor area and volume) as a bedroom. Hence, we set $V_1 = 228.3$ m^3 and $V_2 = V_3 = 32.6$ m^3. We assume a surface area-to-volume ratio of 3/m (Wallace, 1996), which gives $A_1 = 685.0$ m^2, and $A_2 = A_3 = 97.9$ m^2. We assume that contacts in the living quarters are concentrated in 20% of the surface area of the living quarters (e.g., kitchen, bathrooms, eating and lounging areas), implying that $a_1 = 137.0$ m^2. During the symptomatic period, the infected virus is assumed to shed within a circle with radius 1 m near the bed, which is the distance that coughs and sneezes travel. This circle represents 23.5% of the room's floor surface area, and so we set $a_2 = 0.235(97.9) = 23.0$ m^2.

To compute the ventilation rates, we assume a moderate external air exchange rate in the house of 1.0 air exchanges per hour; e.g., each room has one external window (Heinsohn and Cimbala, 1999); this value is consistent with the 1.1/hr average effective air exchange rate in US houses (Sherman and Matson, 1997). We assume that the air flow rate between a bedroom and the living quarters is 60 m^3/hr if the bedroom door is open and 1 m^3/hr if the door is closed (Miller and Nazaroff, 2001). In our base case, we

assume that the bedroom doors are closed when the bedroom is occupied and open when unoccupied.

The death rate of virus in the air is taken from Fig. 1 of Hemmes et al. (1960), which is based on indoor temperatures and a relative humidity of approximately 30%, which is typical of most of the US in winter months. This death rate is consistent with other experiments (Loosli et al., 1943; Schaffer et al., 1976), but is higher than those reported in Harper (1961). The death rates of virus on porous and nonporous surfaces are taken from the curves for tissues and stainless steel, respectively, in the top plot in Fig. 1 of Bean et al. (1982). Virus drops from $10^{3.3}$ to $10^{0.2}$ TCID_{50}/0.1 mL in 4 hr to get $\mu_p = \frac{1}{4}\ln(10^{3.1}) = 1.78$/hr, and virus drops from $10^{3.5}$ to 10 TCID_{50}/0.1 mL in 48 hr to get $\mu_n = \frac{1}{48}\ln(10^{2.5}) = 0.12$/hr. As expected, these death rates are lower than the rates computed from the data in Table 1 in Bean et al. (1982), which measure the quantity of influenza A virus that was transferred to hands from stainless steel and paper tissues over time, because the latter values incorporate not just the death rate of virus on the surface, but also the transfer efficiency from the surface to the hands. Virus on the hands from stainless steel dropped from $10^{4.5}$ to $10^{1.3}$ TCID_{50}/0.1 mL in 5 min and virus on hands from paper tissues dropped from $10^{3.0}$ to $10^{1.0}$ TCID_{50}/0.1 mL in 5 min (data on p. 49 of Bean et al., 1982), which yield death rates of 88.4/hr and 55.3/hr, respectively. We conservatively assume $\mu_h = 55.3$/hr.

We assume that particle settling is dominated by gravimetric settling, so that the settling rate is the area-to-volume ratio times the gravimetric velocity. We take the area-to-volume ratio to be 3/m (Wallace, 1996) and the gravimetric velocity to be proportional to the diameter squared (Heinsohn and Cimbala, 1999). The average gravimetric velocity was 0.028 ft/min for post-evaporation particles whose diameter had a normal distribution with mean 1.34 μm and standard deviation 0.6 μm (Phelps, 1942), implying that the gravimetric velocity proportionality factor is $\frac{0.028 \text{ ft/min}}{(1.34^2+0.6^2)\mu\text{m}^2}$. Because particles lose half their diameter during evaporation, we need to divide this proportionality factor by 4, giving $\kappa = 0.18$/hr μm^2 after multiplying by the area-to-volume ratio 3/m.

We assume that asymptomatic patients are more apt to cover their sneezes and coughs than symptomatic patients ($p_s = 0.75$ vs. $\tilde{p}_s = 0.5$). Living quarters are roughly evenly divided between locations that have primarily porous materials (lounging areas) and locations with primarily nonporous materials (kitchen, bathrooms), and so we set $p_{n1} = 0.5$. Because bedrooms tend to have more porous material (e.g., bedding) than the living quarters, we assume $p_{n2} = 0.25$. We assume that $p_d = 0.25$ and $\tilde{p}_d = 0.5$, so that one-quarter of the leaked surface virus from the infected's bedroom is disposed of during the presymptomatic period, and one-half during the symptomatic period. We assume that susceptibles are much less apt to wash their hands during the asymptomatic period and caregivers are more likely to wash their hands after a contact in the infected room than in the living quarters during the symptomatic period ($p_{h1} = 0.05$, $\tilde{p}_{h1} = 0.2$, $p_{h2} = 0.5$, where the tilde denotes the value during the symptomatic period).

There are six contact transmission parameters that are difficult to estimate: $\gamma_j, h_j, \theta_j, \beta, \delta$ and A_h. Four of these parameters, h_j, β, γ_j and A_h, only appear in our model (e.g., Eq. (18)) as the product $h_j\beta\gamma_j A_h$, which eases the parameter estimation task. Defining the composite parameter $\phi_j = h_j\beta\gamma_j A_h$, we make an educated guess about the relative values of ϕ_1 and ϕ_2, and then estimate ϕ_1 in Section 3.4. In particular, we assume that there are five main contact locations in the house, with the infected room being one of them, and that each sustained contact occurs in one of these locations and picks up a certain fraction

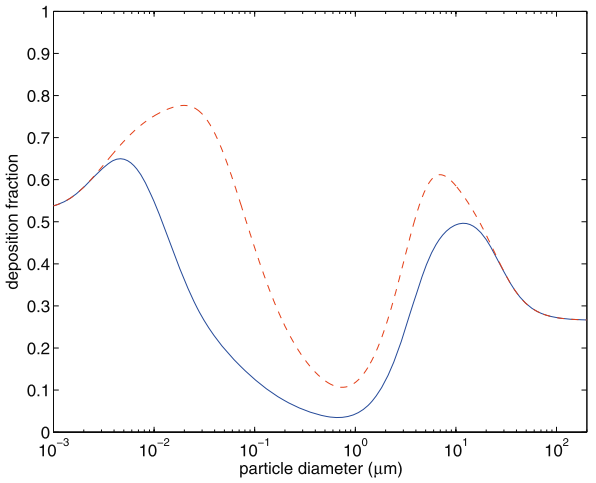

Fig. 3 The deposition function $g(x)$ vs. particle diameter x in the base case, which excludes the anterior nasal passages and the alveolar region (—), and in a possible pandemic scenario, which excludes only the anterior nasal passages (- - -).

of the virus in that location. This implies that $h_2 = 5h_1$. Because the caregiver is likely to have a higher contact rate with the infected during the symptomatic period than during the presymptomatic period, we set $\gamma_2 = 10\gamma_1$, and hence $\phi_2 = 50\phi_1$.

We let $\delta = 0.1$, which includes moving some of the protected virus (e.g., tissues) and unprotected virus (e.g., laundry, cups) out of the infected room. Data on nose-picking have been collected (Hendley et al., 1973), and one of every three people picked their nose in any given hour (i.e., a rate of $\ln(1.5) = 0.405$/hr) when people were seated in an amphitheatre arrangement (so that no one was looking directly at them); the eye-rubbing rate was comparable. The picking rate in a conference arrangement, in which people were facing each other, was approximately 10 times smaller. We assume the self-inoculation rate in the home is $\theta_1 = \theta_2 = 5$/hr, which is approximately six times higher than in the amphitheatre setting.

Susceptibles breathe at rate $b = 20$ m^3/day (Hinds, 1982). We use the deposition model from ICRP (1994) to compute the deposition function $g(x)$. Since the analysis in ICRP (1994) is for airborne particles, the deposition of a particle of diameter x in our analysis corresponds to deposition of a particle of size $\frac{x}{2}$ in the ICRP (1994) model. Using our breathing rate of 20 m^3/day, we have from Fig. D.3 in ICRP (1994) that nasal breathers breathe 100% through the nose and mouth breathers breathe 55% through the nose. Since 4 of 29 subjects in Niinimaa et al. (1980) were mouth breathers, we assume that the fraction of air inhaled through the nose is $\frac{4}{29}(0.55) + \frac{25}{29} = 0.938$. The ciliated columnar epithelial cells are located from the posterior nasal area to the bronchi, and hence we sum the depositions from the head airways region (excluding the anterior nasal passage) and the tracheobronchial region in the deposition model in ICRP (1994) (and linearly interpolate the parameters in Table 15 of ICRP (1994), which gives parameter values for only several breathing rates) to compute our deposition function $g(x)$, which is shown in Fig. 3.

The airborne ID_{50} has been measured to be in the range [0.6,3] $TCID_{50}$ in Alford et al. (1966), which is the amount of nasally-inhaled virus to infect half of humans. Note that our ID_{50}^a has a different interpretation: It is the amount of virus reaching the respiratory epithelium required to infect half of humans. Hence, we cannot use the [0.6, 3] $TCID_{50}$ range directly because we need to account for the facts that some of the inhaled virus does not deposit on the respiratory epithelium and the aerosol sizes (between 1 and 3 μm) used in this study differ from those in Eq. (22) generated by sneezes and coughs. If we use the midway point of the range, 1.8 $TCID_{50}$, and assume that the particle sizes in Alford et al. (1966) were uniformly distributed between 1 and 3 μm, then the total dose delivered to the respiratory epithelium that infects half of humans is

$$ID_{50}^a = 1.8\ TCID_{50} \frac{\int_{1\ \mu m}^{3\ \mu m} x^3 g(2x)\,dx}{\int_{1\ \mu m}^{3\ \mu m} x^3\,dx}, \tag{23}$$

$$= 0.671\ TCID_{50}. \tag{24}$$

We use $g(2x)$, because the airborne particles diameters are quoted in Alford et al. (1966). The nasal ID_{50}^n is taken to be 500 $TCID_{50}$, which is approximately the average of the values 127, 320 and 1,000 $TCID_{50}$ in Couch et al. (1971), Hayden et al. (1996) for nasal inoculation. This nearly three-order-of-magnitude difference between ID_{50}^a and ID_{50}^n plays an important role in our conclusions. These values are from different studies that employ different influenza A strains and different assay procedures (we could not find a study in which the same investigators used the same strain to compare the ID_{50} values of different administration routes), which could account for some of the large difference in ID_{50} values. Consequently, we perform a sensitivity analysis with respect to the ID_{50} values in the Discussion.

3.2. Rhinovirus parameter values

We begin by specifying the rhinovirus parameters. Disease progression is characterized by $T_p = 0.5$ days (Rampey et al., 1992) and $T_I = 12$ days (Rampey et al., 1992), although we incorporate the fact that viral shedding peaks at 48 hr. The death rate in air is $\mu_a = -4\ln(0.0025) = 24.0$/hr (Karim et al., 1985). We use Table 2 of Hendley et al. (1973) for cotton and stainless steel to compute the death rates for porous and nonporous surfaces, respectively, yielding $\mu_p = \ln(10^{1.5}) = 3.45$/hr from time points 0 and 1 hr, and $\mu_n = \frac{1}{3}\ln(10^{0.5}) = 0.38$/hr using time points 0 and 3 hr. The death rate on hands is $\mu_h = -\frac{1}{3}\ln(0.16) = 0.61$/hr (Ansari et al., 1991). The airborne ID_{50} has been measured to be 0.68 $TCID_{50}$ (Couch et al., 1966) based on nasal inhalations of particles between 0.3 and 2.5 μm. As in Eqs. (23), (24), we set

$$ID_{50}^a = 0.68\ TCID_{50} \frac{\int_{0.3\ \mu m}^{2.5\ \mu m} x^3 g(2x)\,dx}{\int_{0.3\ \mu m}^{2.5\ \mu m} x^3\,dx}, \tag{25}$$

$$= 0.216\ TCID_{50}. \tag{26}$$

The $ID_{50}^n = 0.032$ $TCID_{50}$ (Couch et al., 1966), which is the nasal ID_{50}. This value is much lower than the ID_{50} in the mouth (2260 $TCID_{50}$ on the tongue D'Alessio et al.,

1984), which is consistent with the difficulty of oral transmission (D'Alessio et al., 1984; Hendley et al., 1973). Although there are no data on the ID_{50} in the eyes, introduction of the virus on the conjuctival site is believed to be a vehicle for the virus to reach the nose via the nasolacrimal duct, rather than inducing infection of the conjuctiva itself (Winther et al., 1986). Hence, the difference between the nasal and conjunctival ID_{50}s is likely dictated by their relative efficiencies in allowing the virus to get into the nasopharynx.

We obtain the viral shedding parameters as before, but now assuming that the level of virus titers jumps from 3 to 900 $TCID_{50}$/mL during the first 2 days of infection and then drops to 10 $TCID_{50}$/mL on day 7 (Douglas et al., 1966), while the nasal discharge rate for these 3 days are 1, 8 and 1 g/day (Cate et al., 1964). This gives $\nu = 0.5\ln(2400) = 3.89$/day and $\omega = 0.2\ln(720) = 1.32$/day; we assume the shedding rate exponentially increases at rate ν for 2 days and then exponentially decreases at rate ω. We obtain $e^{m_\lambda} = 64.7$ $TCID_{50}$/day by summing the initial sneeze shedding rate of 30 $TCID_{50}$/day (30 TCID/mL, which incorporates 10 mL of nasal wash, times 1 g/day of secretions, divided by 1 g/mL mucus density) and the initial cough shedding rate of 34.7 $TCID_{50}$/day ($e^{-\nu}$ times the peak throat titer of 90 $TCID_{50}$/day, assuming that throat titers are a factor of 10 less than nasal titers (Hendley and Gwaltney, 1988), times the peak cough rate, which is taken to be 70/day (Gwaltney et al., 1978), times the volume per cough, which was already calculated to be 470 droplets per cough times 5.73×10^7 μm^3/droplet). We maintain $e^{\sigma_\lambda} = 40$ as in part (i) of this subsection because $e^{\sigma_X} = 10$ is not inconsistent with the ranges in nasal concentration observed in Meschievitz et al. (1984), Dick et al. (1987), Douglas (1970). We assume the aerosol parameters (d_c, κ) and the physiological parameters $(p(x), b, g(x))$ are the same for rhinovirus and influenza, and we assume the protection fraction and the nonporous fraction for rhinovirus take on the presymptomatic influenza values 0.75 and 0.5, respectively.

3.3. A comparison of rhinovirus and influenza

To motivate why we believe that nearly all influenza transmissions may be via aerosol, we compare the relative routes of transmission across influenza and rhinovirus in the simplified setting where exposure to one infected is in one room of volume V for T time units and the shedding occurs at constant rate λ. For a given λ, the probability of infection satisfies $P_I = 1 - e^{-(c_a + c_s)}$ for an aerosol transmission constant c_a and a contact transmission constant c_s, and we derive mathematical expressions for these two constants. A comparison of these two constants for a particular disease would allow us to quantify the routes of transmission for that disease. Although there are not sufficient data to do this reliably for either influenza or rhinovirus, we can compare the same transmission constant between the two diseases. In particular, using the superscripts rhi and inf for rhinovirus and influenza, we estimate the ratios $\frac{c_a^{\text{inf}}}{c_a^{\text{rhi}}}$ and $\frac{c_s^{\text{inf}}}{c_s^{\text{rhi}}}$, and then draw some insights from their values; these ratios can be numerically estimated because the difficult-to-estimate parameters are common for the two diseases, and cancel out when we consider the ratios. For ease of reference, we include in Table 2 the parameter values that differ between influenza and rhinovirus, which are used to compute the numerical values of these two ratios.

We let $v = \lambda T$ denote the total amount of virus shed by the infected during his infectious period. Equation (9) implies that the air concentration in the room satisfies

$$\dot{C}_a(x,t) = \frac{f(x)(1-p_s)\lambda}{V} - \left[\frac{Q}{V} + \mu_a + \kappa x^2\right] C_a(x,t) \quad \text{for } x \in [0, d_c], \tag{27}$$

Table 2 Influenza vs. rhinovirus comparison

Parameter	Influenza value	Rhinovirus value
Total shed virus	1.93×10^5 TCID_{50}	1.57×10^5 TCID_{50}
ID_{50} for respiratory epithelium	0.671 TCID_{50}	0.216 TCID_{50}
Death rate in air	0.36/hr	24.0/hr
ID_{50} for nose and eyes	500 TCID_{50}	0.032 TCID_{50}
Death rate on porous surfaces	1.78/hr	3.45/hr
Death rate on nonporous surfaces	0.12/hr	0.38/hr
Death rate on hands	55.3/hr	0.61/hr

which with initial condition $C_a(x,0) = 0$ has solution

$$C_a(x,t) = \frac{\frac{f(x)(1-p_s)\lambda}{V}}{\frac{Q}{V} + \mu_a + \kappa x^2}\left(1 - e^{-(\frac{Q}{V} + \mu_a + \kappa x^2)t}\right). \tag{28}$$

Then the total dose from particles of diameter x is

$$D_a(x) = b\int_0^T C_a(x,t)\,dt \quad \text{by Eq. (16)}, \tag{29}$$

$$= \frac{\frac{bf(x)(1-p_s)\lambda}{V}}{\frac{Q}{V} + \mu_a + \kappa x^2}\left(T + \frac{e^{-(\frac{Q}{V} + \mu_a + \kappa x^2)T}}{\frac{Q}{V} + \mu_a + \kappa x^2} - \frac{1}{\frac{Q}{V} + \mu_a + \kappa x^2}\right) \quad \text{by (28)}, \tag{30}$$

$$\approx \frac{\frac{bf(x)(1-p_s)\lambda T}{V}}{\frac{Q}{V} + \mu_a + \kappa x^2} \quad \text{because } T \gg 1 \text{ hr}. \tag{31}$$

That is, the total dose from particles of diameter x is the breathing rate b times the cumulative number of expelled virus in particles of diameter x per unit volume, divided by the total death rate of these particles. Finally, Eqs. (20), (21) and (31) allow us to approximate the aerosol constant by

$$c_a = \frac{\alpha_a b v (1-p_s)}{V}\int_0^{d_c} \frac{f(x)g(x)}{\frac{Q}{V} + \mu_a + \kappa x^2}\,dx. \tag{32}$$

To derive c_s, we use Eqs. (10), (11) and (28) to write the surface virus equations as

$$\dot{C}_p(t) = \frac{p_s + (1-p_s)(1-p_n)\bar{F}(d_c)\lambda}{a} + \frac{(1-p_n)V}{A}\int_0^{d_c} \frac{\frac{f(x)(1-p_s)\lambda}{V}\kappa x^2}{\frac{Q}{V} + \mu_a + \kappa x^2}\left(1 - e^{-(\frac{Q}{V} + \mu_a + \kappa x^2)t}\right)dx - \mu_p C_p(t), \tag{33}$$

$$\dot{C}_n(t) = \frac{(1-p_s)p_n\bar{F}(d_c)\lambda}{a} + \frac{p_n V}{A}\int_0^{d_c} \frac{\frac{f(x)(1-p_s)\lambda}{V}\kappa x^2}{\frac{Q}{V} + \mu_a + \kappa x^2}\left(1 - e^{-(\frac{Q}{V} + \mu_a + \kappa x^2)t}\right)dx - \mu_n C_n(t). \tag{34}$$

Equations (33), (34) can be solved with the integrating factors $e^{\mu_p t}$ and $e^{\mu_n t}$. Discarding lower-order terms (because $e^{-\mu_p T}$ and $e^{-\mu_n T}$ are negligible for realistic values of T) and summing the solutions give

$$C_p(t) + C_n(t) \approx \frac{\lambda}{a}\left(\frac{p_s + (1-p_s)(1-p_n)\bar{F}(d_c)}{\mu_p} + \frac{(1-p_s)p_n\bar{F}(d_c)}{\mu_n}\right) + \frac{\lambda(1-p_s)\kappa}{A}\left(\frac{1-p_n}{\mu_p} + \frac{p_n}{\mu_n}\right)\int_0^{d_c} \frac{f(x)x^2}{\frac{Q}{V} + \mu_a + \kappa x^2}\,dx. \tag{35}$$

By Eqs. (19) and (35) and the identity $v = \lambda T$, we approximate the contact constant by

$$c_s = \frac{\alpha_n v \phi (1-p_h) e^{-\frac{\mu_h}{\theta}}}{a(1-e^{-\frac{\mu_h}{\theta}})}\left[\left(\frac{p_s + (1-p_s)(1-p_n)\bar{F}(d_c)}{\mu_p} + \frac{(1-p_s)p_n\bar{F}(d_c)}{\mu_n}\right) + \frac{a(1-p_s)\kappa}{A}\left(\frac{1-p_n}{\mu_p} + \frac{p_n}{\mu_n}\right)\int_0^{d_c} \frac{f(x)x^2}{\frac{Q}{V} + \mu_a + \kappa x^2}\,dx\right]. \tag{36}$$

Now we substitute parameter values into Eqs. (32) and (36). In the ratio $\frac{c_a^{\text{inf}}}{c_a^{\text{rhi}}}$, the term $\frac{b(1-p_s)}{V}$ in (32) is common to both viruses, and cancels out. We let v be the total amount of shed virus. Because we want the rhinovirus and influenza situations to be as similar as possible, we assume the ratio of the v's is constant even though v itself is random. We take the ratio of the total amount of shed virus to be the ratio of the median of the total amount of shed virus (which is the same as the ratio of the means if we assume the shedding rates for the two diseases are log-normal with the same dispersal factor). By Eq. (8), we have the median shedding rate v_{med}

$$v_{\text{med}} = \int_0^{T_p} e^{m_\lambda} e^{vt}\,dt + \int_{T_p}^{T_s} e^{m_\lambda} e^{vT_p - \omega(t-T_p)}\,dt, \tag{37}$$

$$= \frac{e^{m_\lambda}}{v}\left(e^{vT_p} - 1\right) + \frac{e^{m_\lambda}}{\omega} e^{(v+\omega)T_p}\left(e^{-\omega T_p} - e^{-\omega T_s}\right). \tag{38}$$

The value of v_{med} in (38) is 1.57×10^5 TCID_{50} (assuming $T_p = 2$ days because this is the time of peak viral shedding) for rhinovirus and 1.93×10^5 TCID_{50} for influenza. Although these values may not be accurate, we have used the same method to estimate both, and hence their ratio, which is all that we are interested in, should be reliable. Substituting Eq. (38) into (32) and setting $\frac{Q}{V} = 1/\text{hr}$, we find that the aerosol ratio $\frac{c_a^{\text{inf}}}{c_a^{\text{rhi}}} = 0.77$.

Assuming similar mixing and sanitary behavior in the face of these two viruses, the term $\frac{\phi(1-p_h)}{a}$ is common to both viruses and cancels out in the ratio $\frac{c_s^{\text{inf}}}{c_s^{\text{rhi}}}$. We set $p_s = 0.75$, $p_n = 0.5$, $\frac{Q}{V} = 1/\text{hr}$, and $\frac{a}{A} = 0.2$, substitute (38) into (36) and find that the contact ratio $\frac{c_s^{\text{inf}}}{c_s^{\text{rhi}}}$ equals 4.2×10^{-10}.

The natural measure of the fraction of transmission in disease $k = \{\text{inf}, \text{rhi}\}$ that is due to transmission mode $j = \{a, s\}$ is

$$f_j^k = \frac{1 - e^{-c_j^k}}{2 - \sum_{j=\{a,s\}} e^{-c_j^k}}. \tag{39}$$

While the large difference in the ratios suggests that $f_a^{\text{inf}} > f_a^{\text{rhi}}$, Eq. (39) does not necessarily imply this.

Despite the 9 orders-of-magnitude disparity between $\frac{c_a^{\text{inf}}}{c_a^{\text{rhi}}}$ and $\frac{c_s^{\text{inf}}}{c_s^{\text{rhi}}}$, we cannot directly argue that contact transmission is negligible in influenza, because contact transmission may be very significant in rhinovirus (i.e., c_s^{rhi} could be very large). Consequently, in Appendices A and B we reanalyze several sets of rhinovirus transmission experiments carried out by the University of Wisconsin research group. In Appendix A, we analyze data from Dick et al. (1987), in which susceptibles were physically restricted from touching their hands to their face (thereby disallowing contact transmission) while playing cards with infecteds. Using our airborne transmission model (i.e., Eq. (21) with $\alpha_n = 0$) and the actual number of susceptibles who were infected, we estimate the rhinovirus median shedding rate e^{m_λ}. In Appendix B, we analyze data from six rhinovirus experiments in which susceptibles and infecteds mixed freely in a closed room, thereby allowing all modes of transmission (Meschievitz et al., 1984). We find that the airborne experiments in Dick et al. (1987) and six of the seven experiments in Meschievitz et al. (1984) all fit the airborne model $P_I = 1 - e^{-\frac{cT}{V}}$, where T is the infected hours of exposure and V is the room volume, raising the possibility that nearly all transmission in Meschievitz et al. (1984) was due to aerosol.

The analyses in Appendices A and B are suggestive of the dominance of aerosol transmission for rhinovirus, but are hardly convincing: the number of subjects in each experiment is small, the data are insufficient to reliably estimate the viral shedding rate of each experimental subject, the experimental conditions are somewhat contrived, and the University of Virginia research group (Hendley and Gwaltney, 1988) has shown via iodine treatment on fingertips that contact transmission plays a nontrivial role in the rhinovirus transmission between mothers and their children in a natural setting. Hence, in Section 3.4 we take a different approach for estimating the value of rhinovirus ϕ that is motivated by our comparison in Section 3.3, which is to construct an upper bound for ϕ using empirical rhinovirus values for the secondary attack rate in the home. This analysis also reveals an inconsistency (on the order of 2–4 orders of magnitude) between the first-principles estimate of the median viral shedding rate and the estimate based on backing it out from the proportion of people infected. This could be because the first-principles estimate may be based on cough and sneeze data from healthy people.

3.4. Bounding ϕ using rhinovirus SAR

We now move away from the experimental settings in Meschievitz et al. (1984) and Dick et al. (1987), and equate the empirical rhinovirus values for the secondary attack rate (SAR) in the home with the probability of infection P_I predicted by our model using the data in Sections 3.1, 3.2. Before specifying our bounding procedure, we describe how our model is adapted to the nonexperimental setting. We assume that the infected and

susceptible spend 12 hours together at home, with $\Delta_1 = 4$ hr making contact in the living quarters and $\Delta_2 = 8$ hr sleeping in separate bedrooms; the infected does not withdraw to his bedroom during the symptomatic period. That is, we change the indicator functions from those in Eqs. (1)–(7) to

$$I_{11}(t) = I_{21}(t) = \begin{cases} 1 & \text{for } t \in [(24i + \tau_1)^+, \min\{(24i + \tau_1 + \Delta_1)^+, T_I\}) \\ & \quad \text{for } i = -1, \ldots, \frac{T_I}{24} - 1, \\ 0 & \text{otherwise,} \end{cases} \tag{40}$$

$$I_{12}(t) = I_{23}(t) = \begin{cases} 1 & \text{for } t \in [\min\{(24i + \tau_1 + \Delta_1)^+, T_I\}, \\ & \qquad \min\{(24i + \tau_1 + \Delta_1 + \Delta_2)^+, T_I\}) \\ & \quad \text{for } i = -1, \ldots, \frac{T_I}{24} - 1, \\ 0 & \text{otherwise.} \end{cases} \tag{41}$$

The predicted probability of infection P_I can vary $\pm 5\%$ depending upon the value of τ_1, and we set $\tau_1 = 18$ hr, which generates a P_I value that is roughly midway between the two extremes in Fig. 4a. For example, this set-up is consistent with the infectious period beginning at midnight, and people being out of the house during 6 a.m.—6 p.m., in the living quarters during 6–10 p.m., and in their bedroom during 10 p.m.—6 a.m.

Turning to the bounding procedure, we recall that our analyses in Appendices A and B were unable to derive an accurate estimate for the fraction of rhinovirus transmission that is via aerosol, a quantity we denote by f_a. By Eq. (21), the natural quantity to take as the predicted fraction of transmissions that are aerosol is

$$f_a = \frac{1 - \int_0^\infty e^{-\alpha_a \bar{D}_a(\lambda)} h(\lambda)\, d\lambda}{2 - \int_0^\infty e^{-\alpha_a \bar{D}_a(\lambda)} h(\lambda)\, d\lambda - \int_0^\infty e^{-\alpha_n \bar{D}_s(\lambda)} h(\lambda)\, d\lambda}. \tag{42}$$

We also do not have accurate estimates for e^{m_λ} and ϕ in the natural setting. In addition, the SAR values in the literature vary: The SAR from a 1983 study in Tecumseh, MI (Tables 2 and 4 in Rampey et al., 1992) was 0.133, and larger values have been estimated in large Seattle studies focused on families with grade-school children (0.28) (Fox et al., 1985) or preschool children (0.44) (Fox et al., 1975). Another reason for the discrepancy in SAR values is that, unlike the Seattle studies, Rampey et al. (1992) only obtained specimens from people who self-reported symptoms.

Our bounding procedure estimates two parameters, e^{m_λ} and ϕ, with two equations, and maximizes ϕ by allowing liberal ranges for the values of the parameters f_a and SAR. The first of these two equations sets the empirical SAR equal to the probability of infection P_I predicted by our model using the data in Section 3.2, and the second equates the specified fraction of rhinovirus transmissions that is via aerosol to the value predicted in Eq. (42). Figure 4b shows the values of e^{m_λ} and ϕ for SAR $\in [0.15, 0.45]$ and $f_a = 0.1$, 0.5 and 0.9. We use Fig. 4b to obtain an upper bound on ϕ by solving

$$\max_{f_a, \text{SAR}, e^{m_\lambda}, \phi} \quad \phi \tag{43}$$

$$\text{subject to} \quad f_a \in [0.1, 0.9], \tag{44}$$

$$\text{SAR} \in [0.15, 0.45], \tag{45}$$

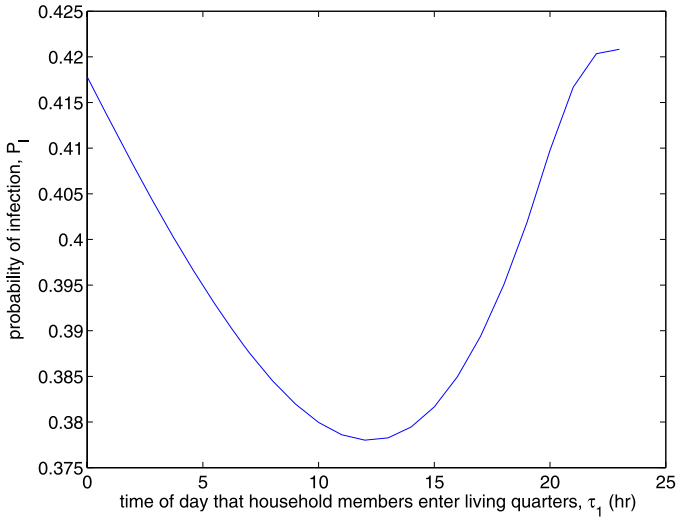

(a)

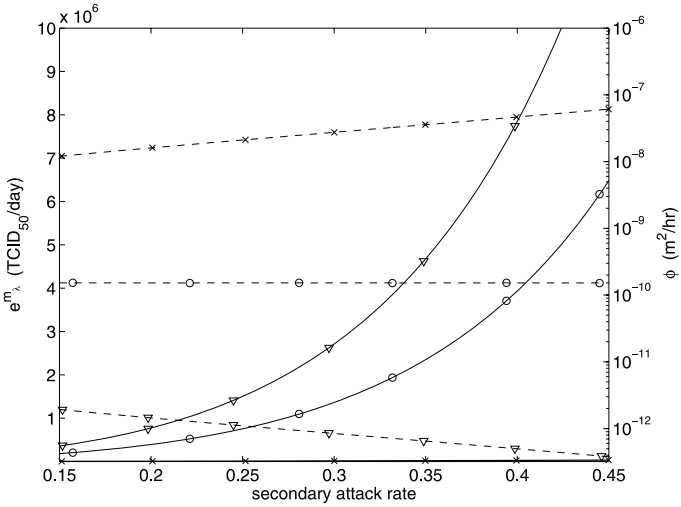

(b)

Fig. 4 Rhinovirus. (a) For $e^{m_\lambda} = 7.5 \times 10^6$ TCID$_{50}$/day and $\phi = 0$, the probability of rhinovirus infection vs. the time of day that household members enter the living quarters (τ_1), where $\tau_1 = 0$ corresponds to the same time of day that the infectious period begins. (b) Fixing $\tau_1 = 18$ hr, we plot e^{m_λ} (—) and ϕ (- - -) vs. SAR for $f_a = 0.1$ ($\times$), 0.5 ($\circ$) and 0.9 ($\triangledown$). These curves are employed in the optimization problem (43)–(45).

and subject to e^{m_λ} and ϕ falling on the appropriate curves in Fig. 4b. The solution to this optimization problem is $f_a = 0.1$, SAR $= 0.45$, $e^{m_\lambda} = 3.22 \times 10^4$ TCID$_{50}$/day, and $\phi = 6.1 \times 10^{-8}$ m^2/hr. Although we round this bound up and set $\phi_1 = 1 \times 10^{-7}$ m^2/hr in our influenza model, we emphasize that this upper bound is probably much greater than the true value.

Finally, the e^{m_λ} estimate of 1.19×10^9 TCID_{50}/day in Appendix A is not directly comparable to the values in Fig. 4b for two reasons. The parameter e^{m_λ} represents the original viral shedding rate in Fig. 4b, whereas in Dick et al. (1987) it corresponds to the median shedding rate of the 8 out of 30 people with the most severe symptoms, where these 30 people may have been shedding at close to their peak rate. If $X_1, \ldots, X_{30}$ are independent and identically distributed (iid) log-normal random variables with $e^{\sigma_\lambda} = 50$ and unknown median e^{m_λ}, and if we let $\text{Med}[X_{\{n:30\}}]$ denote the median of the nth largest of these 30 random variables, then an order statistics analysis shows that $\frac{e^{m_\lambda}}{\text{Med}[X_{\{4.5:30\}}]} = 0.013$, regardless of the value of e^{m_λ}. The conversion factor from peak to initial shedding is $e^{-2(3.89)}$, and the factor is $e^{-3.89}$ if the subjects in Dick et al. (1987) were 24 hr from their peak shedding time. Combining these factors, we see that 1.19×10^9 TCID_{50}/day corresponds to 6.47×10^3 TCID_{50}/day if the subjects were at their peak shedding, and corresponds to 3.16×10^5 TCID_{50}/day if they were 24 hr from their peak shedding time. This latter value corresponds to the low end of the SAR range in Fig. 4b.

A detailed analysis of the model used in this subsection (data not shown) reveals that nearly all infections occur while the infected and susceptibles are together in the living quarters (the virus concentration in the living quarter's air is approximately 100-fold larger when the infected is present than when he is absent), most transmissions are caused by infecteds with unusually high shedding rates (consistent with D'Alessio et al., 1976), and $\approx$80% of transmissions occur during the 4-hr mixing period that is closest to the time of the peak shedding rate (i.e., 48 hours into the infectious period). Moreover, due to the rapid death rate of virus in the air, there is virtually no effect on contact transmissions from ventilation, intercompartmental air flow or settling.

3.5. Interpandemic influenza

In this subsection, we estimate the value of our last remaining parameter, the median viral shedding rate e^{m_λ}, using the interpandemic influenza SAR, which allows us to quantify the aerosol and contact routes of transmission for interpandemic influenza. We alter the model in Section 2 to reflect an interpandemic situation, and use the parameter values in Table 1 except as specified in this paragraph. We set ϕ_1 equal to the upper bound 1×10^{-7} m^2/hr for ϕ from Section 3.4, assuming similar presymptomatic behavior for influenza and rhinovirus (and similar capabilities of recovering virus from the environment, which is one of the factors affecting the parameter h_j—for both viruses, the virus dries in 5–20 minutes on surfaces and can be recovered from these surfaces by hands, albeit with difficulty, after drying Bean et al., 1982, Hendley et al., 1973, Ansari et al., 1991). We also need to change the time durations Δ_1 and Δ_2 to represent an interpandemic setting. In particular, we assume the infected still withdraws to his bedroom during the symptomatic period and receives $\Delta_3 = 1$ hr of care from a caregiver per day, but assume all susceptibles spend $\Delta_1 = 4$ hr in the living quarters, $\Delta_2 = 8$ hr in his bedroom, and 12 hr out of the house, as in the rhinovirus case in Eqs. (40), (41). That is, Eqs. (1)–(7) still hold, but with $\Delta_1 = 4$ hr and $\Delta_2 = 8$ hr; the parameters τ_1 and τ_3 are specified later. To better capture interpandemic behavior, we also reduce the virus disposal fraction $\tilde{p}_d$ in Table 1 from 0.5 to 0.25 during the symptomatic period and reduce the handwashing probabilities $(p_{h1}, \tilde{p}_{h1}, p_{h2})$ from $(0.05, 0.2, 0.5)$ to $(0.05, 0.05, 0.2)$.

Because of the unreliability of our estimate $e^{m_\lambda} = 1748$ TCID_{50}/day from Section 3.1, we treat e^{m_λ} as an unknown. We solve for this parameter by assuming that the interpandemic influenza SAR is $\frac{1}{6}$ (Longini and Koopman, 1982). The interpandemic influenza

SAR values in the literature vary widely, with some values in the 0.13–0.15 range, and others at 0.38 (Carrat et al., 2002) (which drops to 0.362 after accounting for coinfections Ferguson et al., 2005) and even higher (Carrat et al., 2002). Although the degree of population immunity plays a role in the SAR, one of the main reasons for this heterogeneity is the differences in how a case is defined: the higher values include low-grade illnesses (e.g., with no fever) and do not obtain lab confirmation of influenza (Carrat et al., 2002), and the lower numbers require severe symptoms that do not include more than one-third of the lab-confirmed cases. Hence, our SAR is near the lower end of the empirical range, which is also consistent with our assumption that all infecteds withdraw to the bedroom (i.e., have severe symptoms).

In our model, SAR represents the weighted average infection probability (directly from the infected) of susceptible household members, which is $\frac{2P_{I2}+P_{I3}}{3}$. The values of P_{I2} and P_{I3} vary with the time of day that the household members gather in the living quarters (τ_1) and the time of day that the caregiver initiates care (τ_3), and we choose the base-case values $\tau_1 = 13$ hr and $\tau_3 = 11$ hr (Fig. 5a), which achieve typical infection probabilities; e.g., we can think of the infection beginning at 5 a.m., people mixing in the living quarters during 6–10 p.m., and the caregiver providing care during 4–5 p.m. Solving $\frac{2P_{I2}+P_{I3}}{3} = \frac{1}{6}$ using this model gives $e^{m_\lambda} = 2.88 \times 10^7$ TCID_{50}/day, which is 4 orders-of-magnitude larger than the first-principles estimate from Section 3.1. With these base-case values, the infection probabilities are $P_{I2} = 0.109$ and $P_{I3} = 0.282$ (Figs. 5b and 5c), so that the caregiver is more than twice as likely to get infected as the noncaregiver. Also, the fraction of infections due to contact transmission is 7.0×10^{-4}, and 52.7% of transmissions occur in the presymptomatic period, which is slightly higher than the 0.3–0.5 estimate in Fraser et al. (2004).

To provide a sense for how far our parameter values could be pushed before the amount of contact transmission becomes nontrivial, we assume that the caregiver transfers no surface virus to the living quarters ($\delta = 0$), which maximizes contact transmission because the caregiver incurs nearly all of the contact transmission, and symptomatics never wash their hands ($p_h = \tilde{p}_{h1} = \tilde{p}_{h2} = 0$). With these extreme changes, we would need to increase $\frac{\phi_2}{\phi_1}$, which is the ratio of the composite surface contact rate during the symptomatic and pre-symptomatic periods, from 50 to 6.6×10^4 to achieve the level of 10% of all infections being via contact transmission.

3.6. Pandemic influenza

With all of the parameter values in hand, we return to the pandemic influenza model and assess the relative importance of the aerosol and contact routes of transmission. We assume less time outside the home in the pandemic setting (Homeland Security Council, 2006; Markel et al., 2006; Barry, 2004) and let $\Delta_1 = 8$ hr and $\Delta_2 = 12$ hr. We again let $\tau_1 = 13$ hr and $\tau_3 = 11$ hr, which also achieve typical infection probabilities for the pandemic case. Running our model in Section 2 with the pandemic parameters yields $P_{I2} = 0.176$ and $P_{I3} = 0.296$.

In the base-case pandemic version of the model, the fraction of infections due to contact transmission is 3.7×10^{-4} and the fraction of infections during the presymptomatic period increases from 0.527 to 0.637 because the noncaregiving susceptibles receive a higher presymptomatic dose. For ease of reference, Table 3 contains a comparison of the main characteristics of the interpandemic and pandemic versions of the model. We

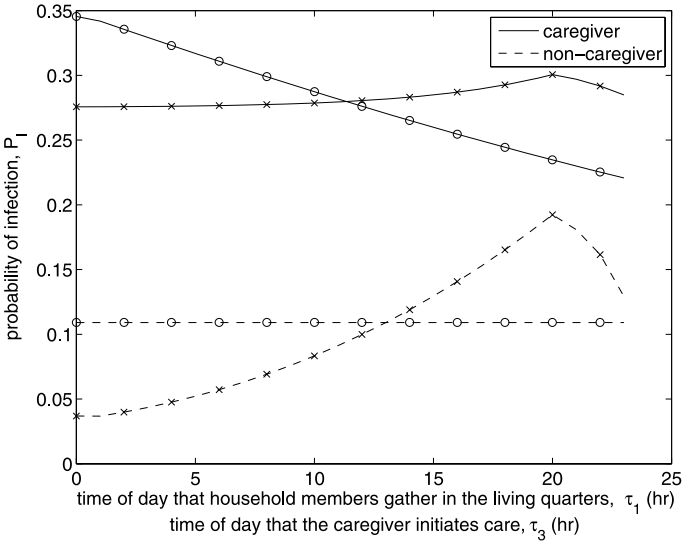

(a)

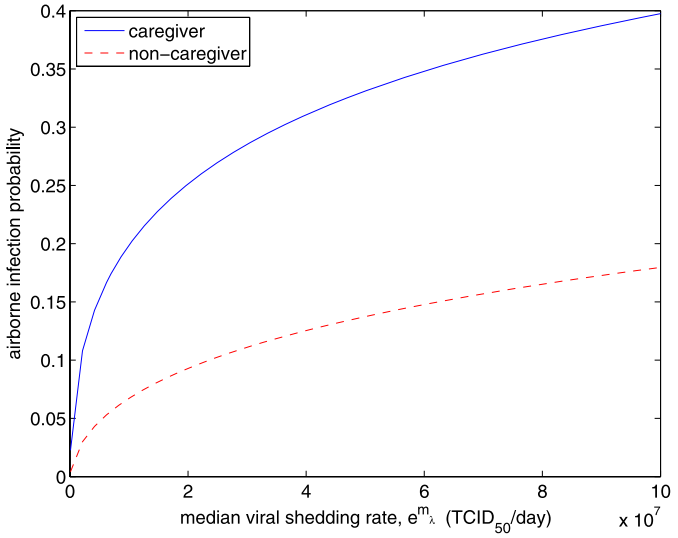

(b)

Fig. 5 Interpandemic influenza. (a) For $e^{m_\lambda} = 2.88 \times 10^7$ TCID_{50}/day and $\phi = 1 \times 10^{-7}$ m^2/hr, the probability of infection for the caregiver (—) and non-caregiving susceptibles (- - -) vs. τ_1 with $\tau_3 = 11$ hr ($\times$), and vs. τ_3 with $\tau_1 = 13$ hr ($\circ$). (b) Aerosol infection probability and (c) contact infection probability vs. the median viral shedding rate e^{m_λ} for $\phi = 1 \times 10^{-7}$ m^2/hr, $\tau_1 = 13$ hr and $\tau_3 = 11$ hr.

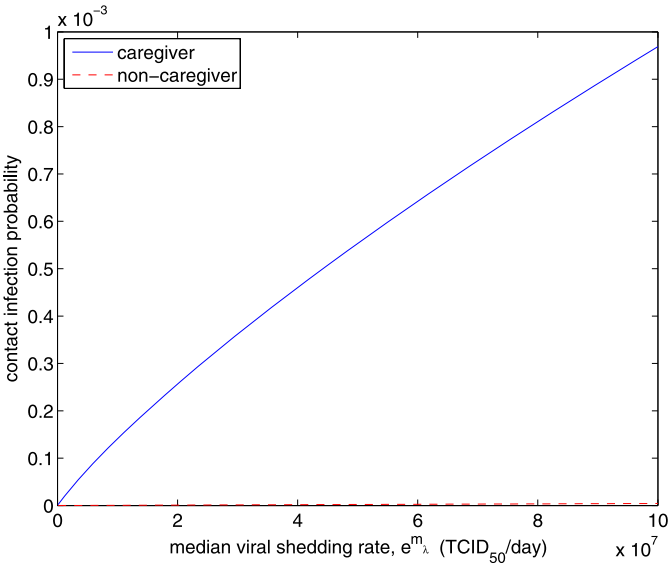

(c)

Fig. 5 (*Continued.*)

Table 3 Comparison of interpandemic and pandemic influenza

Parameter	Description	Interpandemic	Pandemic
Δ_1	hr/day in living quarters	4	8
SAR	Secondary attack rate	0.167	0.216
$1 - f_a$	Fraction contact transmission	7.0×10^{-4}	3.7×10^{-4}
	Fraction pre-symptomatic	0.527	0.637
$\frac{P_{I2}}{P_{I3}}$	$\frac{\text{caregiver infection probability}}{\text{non-caregiver infection probability}}$	2.58	1.68

also display the virus concentration in the air of the three compartments, $\int_0^\infty C_{ai}(x,t)\,dx$, throughout the infectious period in the pandemic base case (Fig. 6).

4. Close expiratory transmission

In the household model analyzed in Section 2, it is implicitly assumed that the infected sheds virus into the environment (either into the air or onto surfaces) and then the virus is transferred from the environment to the susceptible (either through inhalation or contact). However, it is important to look at situations where expelled virus travels directly to the susceptible. This can only occur when the infected and susceptible are facing each other in close proximity, and the lack of data on the frequency of close expiratory events makes it very difficult to incorporate this explicitly into a general household model. Instead, in this section, we estimate the probability of infection due to an isolated close-range cough or sneeze.

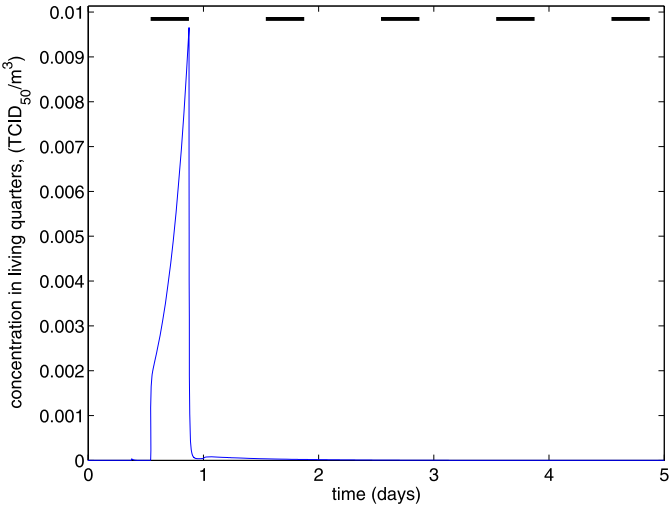

(a)

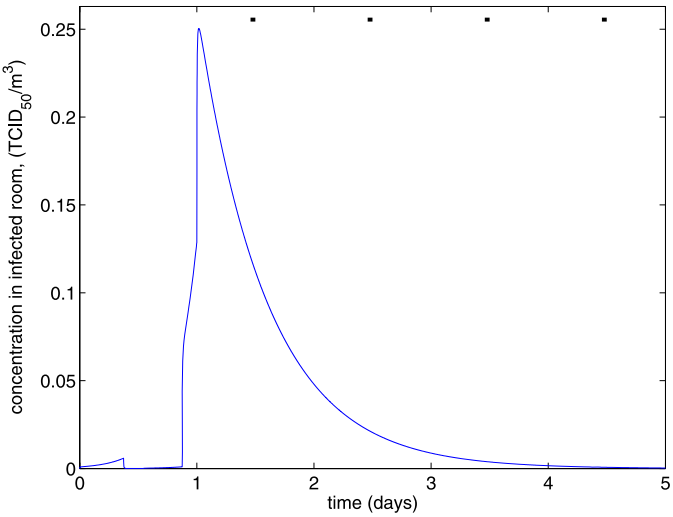

(b)

Fig. 6 Virus concentration in the air. In the pandemic influenza base case, the virus concentration in the air throughout the infectious period in the (a) living quarters, (b) infected's bedroom, (c) susceptible's bedroom. The solid lines across the top represent the times when the susceptible(s) are in the compartment.

We look at three different transmission routes during these close expiratory events. If an infected takes a breath immediately after a sneeze or cough, then he may inhale some of the virus. As in the household model, we look at inhalation of particles in the $<$20 μm range (preevaporation). We also analyze the potential inhalation of particles in

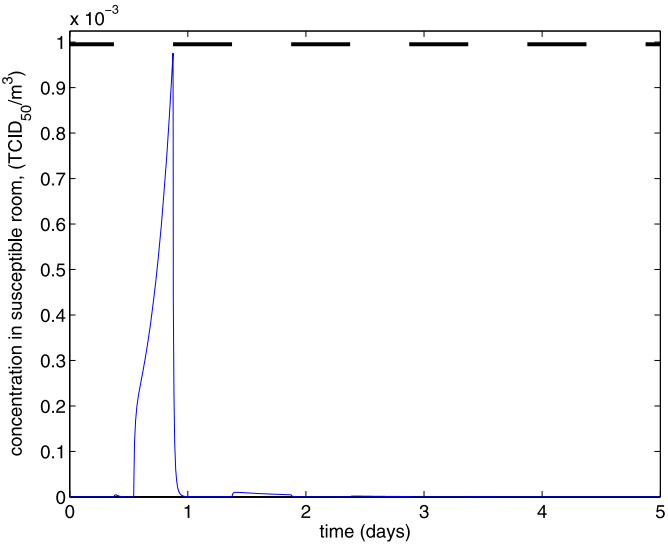

(c)

Fig. 6 (*Continued.*)

the [20, 200] μm range: while these particles settle rapidly to surfaces, a breath right after a cough or sneeze may inhale these particles before settling occurs. Finally, we analyze droplet transmission, where large particles from a sneeze or cough land on the mucous membranes of the nose or eyes. The analysis in this section is similar to Section 5 in Nicas and Sun (2006).

To model transmission from a close sneeze or cough, we assume the susceptible and infected are at the same height, the sneeze or cough particles emanate horizontally in a spherical cone-shaped region with a total angle of 90° (Fig. 2 in Wells, 1955), and the distance between the two people is 60 cm. We take a similar approach to Nicas and Sun (2006) and look at individual particles rather than just the emitted virus. We assume the particles disperse in a uniform manner in the cone emanating from the infected's face, but because only a handful of the particles carry the majority of the virus, we cannot assume that the virus also distributes uniformly in this cone. We need to determine how many particles hit the infection target zone (either the epithelium or the nose or eyes) and how much virus is contained on each of these particles.

We compute the dose from the respirable particles (i.e., $<$20 μm) in Section 4.1, the dose from the inspirable particles (i.e., in the [20, 200] μm range) in Section 4.2, and the dose from droplet transmission in Section 4.3. These doses are mnemonically defined to be D_r, D_i, and D_d, respectively. The infection probability from a cough or sneeze is calculated in Section 4.4. In Section 4.5, we compare the contribution from the three routes of transmission to determine which is dominant for influenza, and also derive the influenza-to-rhinovirus ratios for these three modes of transmission, as we did in Section 3.3.

4.1. *Respirable transmission*

We assume that the expiratory event releases λ TCID_{50} of virus and N particles, a certain fraction of which are respirable, i.e., <20 μm. Hence, a cough or sneeze releases $N\int_0^{20} p(x)\,dx$ respirable particles, and we follow the analysis of inspirable (not respirable) particles in Nicas and Sun (2006) and assume that these particles spread out uniformly in the spherical cone-shaped region that emanates from the infected's face (actually, Section 5.2 of Nicas and Sun, 2006 assumes that both the particles and the virus distribute uniformly), and the susceptible takes one inhaled breath of air from this cone. The volume of the cone (which includes the spherical cap) when the infected and susceptible are 60 cm apart is

$$V_{\text{cone}} = \frac{1}{3}\pi 60\cos\left(\frac{\pi}{4}\right)\left(60\sin\left(\frac{\pi}{4}\right)\right)^2 + \frac{1}{3}\pi\left(60-60\cos\left(\frac{\pi}{4}\right)\right)^2\left(120+60\cos\left(\frac{\pi}{4}\right)\right). \tag{46}$$

The breathing rate is $\frac{10^6 b}{24}$ cm^3/hr and we assume 12 breaths per minute (Hinds, 1982). Thus, the probability that any given particle is inhaled by the infected (assuming the susceptible only breathes air in the cone) is $\frac{10^6 b}{24\times 12\times 60\times V_{\text{cone}}}$. Only a fraction $g(x)$ of the inhaled particles of size x will deposit in the epithelium. Taken together, we use the Poisson approximation to the binomial and model the total number of particles, N_r, that reach the target region as a Poisson random variable with mean

$$\frac{10^6 b}{24\times 12\times 60\times V_{\text{cone}}}\int_0^{20}\frac{p(x)}{\int_0^{20}p(y)\,dy}g(x)\,dx\left(N\int_0^{20}p(x)\,dx\right). \tag{47}$$

For $j=1,\ldots,N_r$, let $D_r(j)$ be iid random variables that represent the dose in a particle that reaches the epithelium. Then $D_r(j)$ takes on the value $\frac{\lambda f(x)}{Np(x)}$ (which equals $\frac{\lambda x^3}{N\int_0^\infty x^3 p(y)\,dy}$ by the definition of $f(x)$) according to the pdf $\frac{p(x)g(x)}{\int_0^{20}p(y)g(y)\,dy}$, and the total dose due to respirable transmission is

$$D_r = \sum_{j=1}^{N_r} D_r(j), \tag{48}$$

which is a random sum of random variables.

We conclude this subsection by noting that the assumption that the respirable particles distribute uniformly in the cone is highly suspect. The distance that a particle will travel depends on the size of the particle and the velocity of the sneeze or cough. In this subsection and in Sections 4.2 and 4.3, we use the particle motion model on pages 604–615 of Heinsohn and Cimbala (1999) (more specifically, we numerically integrate Eq. (8–76) on page 611 of Heinsohn and Cimbala, 1999) to compute the stopping distances (i.e., the distances that expelled particles will travel) of particles of various sizes. We find that 20 μm particles (measured preevaporation) have a stopping distance of 0.3 cm if emitted with a coughing speed of 12.5 m/s (Khan et al., 2004), and have a stopping distance of 1.3 cm if

emitted with a sneezing speed of 100 m/s (Wells, 1955). Hence, despite what Eqs. (46)–(48) predict (the results are reported in Section 4.4), it appears that respirable particles will not be distributed uniformly throughout the cone and that the susceptible will not inhale these particles during his first breath. Of course, these particles remain in the air for some time and may be inhaled by the susceptible in subsequent breaths, although we view such inhalation as being part of the aerosol transmission modeled in Section 2.

4.2. Inspirable transmission

Particles in the [20, 200] μm range ordinarily settle quickly to surfaces. However, after a close cough or sneeze, the susceptible may inhale some of these particles during his first breath, and some of these particles deposit in the epithelium of the extrathoracic airway, which is captured by the deposition function $g(x)$. Assuming that inspirable particles distribute uniformly throughout the cone (as in Section 5.2 in Nicas and Sun, 2006), we mimic Section 4.1 and find that the total dose due to inspirable transmission, D_i, is given by

$$D_i = \sum_{j=1}^{N_i} D_i(j), \tag{49}$$

where N_i is a Poisson random variable with mean

$$\frac{10^6 b}{24 \times 12 \times 60 \times V_{\text{cone}}} \int_{20}^{200} \frac{p(x)}{\int_{20}^{200} p(y)\,dy} g(x)\,dx \left(N \int_{20}^{200} p(x)\,dx \right), \tag{50}$$

and $D_i(j)$ are iid random variables taking on the values $\frac{\lambda f(x)}{N p(x)}$ according to the pdf $\frac{p(x)g(x)}{\int_{20}^{200} p(y)g(y)\,dy}$.

Using Eq. (8–76) of Heinsohn and Cimbala (1999), we find that the stopping distance for a 200 μm particle is 15 cm for a cough and 48 cm for a sneeze. Hence, our analysis predicts that despite the results in Section 4.4 pertaining to (49), (50), inspirable particles from a cough will not travel far enough to be inhaled by the susceptible in his first breath. Because the stopping distance of 48 cm is close to the presumed intersubject distance of 60 cm, it seems possible that a small fraction of the largest inspirable particles from a sneeze could be inhaled in the susceptible's first breath.

4.3. Droplet transmission

Finally, we look at droplet transmission, in which virus in large particles deposit directly onto the mucous membranes of the nose and eyes, rather than on the epithelium of the airways. Whether or not a particle can travel the 60 cm between the susceptible and the infected depends on the velocity of the event and the size of the particle. Using Eq. (8–76) in Heinsohn and Cimbala (1999), we find that particles <488 μm will travel <60 cm if emitted from a cough, and hence will not contribute to droplet transmission; similarly, particles <232 μm will travel <60 cm if emitted from a sneeze. We define the

minimum particle size that can contribute to droplet transmission by $\bar{d}$, which is equal to 488 μm for a cough and 232 μm for a sneeze.

The target is the eyes and nose (as mentioned in Section 2.2, we ignore deposition on the mouths and lips), and we assume the surface area of the open eyes (6 cm^2) and nostrils (2 cm^2) is 8 cm^2. We assume that emitted particles travel uniformly in a circle at the top of an increasing spherical cone with a total angle of 90° from the infected to the susceptible. The area of this surface when the infected and susceptible are y cm apart is computed using the area of a spherical cap, $2\pi y(y - y\cos(\frac{\pi}{4}))$. Thus, we would expect a fraction, $\frac{8}{2\pi 60(60-60\cos(\frac{\pi}{4}))} = 1.2 \times 10^{-3}$, of the expelled particles to hit the target of the eyes and nose, and therefore we model the total number of particles to hit the target region as a Poisson random variable with mean (recall from Eq. (22) that the maximum particle size is 4,000 μm)

$$\frac{8}{2\pi 60(60 - 60\cos(\frac{\pi}{4}))}\left(N \int_{\bar{d}}^{4000} p(x)\,dx\right). \tag{51}$$

As in Sections 4.1 and 4.2, the total dose is

$$D_d = \sum_{j=1}^{N_d} D_d(j), \tag{52}$$

where $D_d(j)$ are iid random variables taking on the values $\frac{\lambda f(x)}{Np(x)}$ according to the pdf $\frac{p(x)}{\int_{\bar{d}}^{4000} p(y)\,dy}$.

4.4. Infection probability

Given the three doses, D_r, D_i, D_d, we can compute the infection probability

$$1 - \mathbf{E}\left[e^{-(\alpha_a D_r + \alpha_a D_i + \alpha_n D_d)}\right]. \tag{53}$$

The expectation in Eq. (53) involves 3 layers of randomness: the number of particles that hit the target zones of infection (N_r, N_i, N_d) is Poisson, the dose in a particle $(D_r(j), D_i(j), D_d(j))$ is a function of the size of the particles, which has pdf $p(x)$, and the shedding rate λ determines the dose per particle and is log-normal with pdf $h(\lambda)$.

We are now in a position to compute the infection probability from one sneeze and one cough. To be consistent with our primary model, we use an initial shedding rate of 2.88×10^7 $TCID_{50}$/day, which is several orders of magnitude greater than the estimate from first principles. We assume 99% of this shedding comes from sneezes and 1% from coughs, with the daily shedding coming equally from each sneeze or cough. We take 360 coughs/day for pneumonia patients (Loudon and Brown, 1967) and we use 11 sneezes/day from one of the rhinovirus experiments (Dick et al., 1987). We set $N = 470$ for a cough (Loudon and Roberts, 1967) and $N = 94000$ for a sneeze because there were 200 times more particles in a sneeze than a cough in Duguid (1946).

We compute the median shedding of a sneeze and cough at the time of peak shedding to be

$$\left(0.99 \times e^{4.94} \times 2.88 \times 10^7 \frac{\text{TCID}_{50}}{\text{day}}\right)\left(\frac{1}{11}\frac{\text{day}}{\text{sneeze}}\right) = 3.62 \times 10^8 \frac{\text{TCID}_{50}}{\text{sneeze}}, \quad (54)$$

$$\left(0.01 \times e^{4.94} \times 2.88 \times 10^7 \frac{\text{TCID}_{50}}{\text{day}}\right)\left(\frac{1}{360}\frac{\text{day}}{\text{cough}}\right) = 1.12 \times 10^5 \frac{\text{TCID}_{50}}{\text{cough}}. \quad (55)$$

Letting the shed virus $h(\lambda)$ be the log-normal pdf with medians as in (54), (55) and $e^{\sigma_\lambda} = 10$ (because we are considering a single sneeze or cough, we only include the dispersion from the viral concentration), we compute the infection probability from (53), which is 0.9999 for a sneeze and 0.244 for a cough.

We also compute the infection probability from an event that occurs at an off-peak time. The virus concentrations shed from a sneeze at 12 hours before and after the peak shedding time are 3.06×10^7 and 1.55×10^8 TCID_{50}, respectively, and the resulting infection probabilities at these times are 0.996 and 0.999. The virus concentrations shed from a cough at 12 hours before and after the peak shedding time are 9.46×10^3 and 4.78×10^4 TCID_{50}, respectively, and the resulting infection probabilities at these times are 0.125 and 0.202.

These probabilities are the conditional probabilities of infection from a sneeze or cough given that the infected is directly in front of a susceptible. To determine the unconditional probability, we would need to multiply these conditional probabilities by the probability that the susceptible is directly in front of the infected when the infected sneezes or coughs (see Nicas and Sun, 2006 for example calculations). Even if the unconditional probabilities of infection are several orders of magnitude less than the conditional probabilities given above, we have analyzed only one cough or sneeze. The total probability of infection from close expiratory events taken over all coughs and sneezes may be nontrivial even if the probability of infection from one cough or sneeze is very small (see Nicas and Sun, 2006 for example calculations).

4.5. Comparison

To compare these three routes of transmission, we define the fraction of transmission, similar to Eq. (42), to be

$$f_r = \frac{1 - \mathbf{E}[e^{-\alpha_a D_r}]}{3 - \mathbf{E}[e^{-\alpha_a D_r} + e^{-\alpha_a D_i} + e^{-\alpha_n D_d}]}, \quad (56)$$

$$f_i = \frac{1 - \mathbf{E}[e^{-\alpha_a D_i}]}{3 - \mathbf{E}[e^{-\alpha_a D_r} + e^{-\alpha_a D_i} + e^{-\alpha_n D_d}]}, \quad (57)$$

$$f_d = 1 - f_r - f_i. \quad (58)$$

During peak shedding, the values are $f_r = 0.28$, $f_i = 0.36$, and $f_d = 0.35$ for a sneeze and $f_r = 0.04$, $f_i = 0.91$, and $f_d = 0.04$ for a cough. Consequently, inspirable transmission dominates during a cough and all three modes of transmission are sufficiently potent for a sneeze.

However, if we assume, as suggested by the stopping distance calculations in Sections 4.1–4.3, that respiratory and inspirable transmission do not occur during the first

breath, then the probability of infection—which is due entirely to droplet transmission—is 0.981 for a sneeze and 0.011 for a cough.

As in Section 3.3, we investigate the influenza-to-rhinovirus ratios of these three routes of transmission. Given the doses from the three routes, the probability of infection from a direct sneeze or cough follows $P_I = 1 - e^{-(c_r + c_i + c_d)}$. From Section 4.1 to Section 4.3, we have $c_r = \alpha_a D_r$, $c_i = \alpha_a D_i$, and $c_d = \alpha_n D_d$. As in Section 3.3, we add superscripts for influenza and rhinovirus, and are interested in the ratios $\frac{c_r^{\text{inf}}}{c_r^{\text{rhi}}}$, $\frac{c_i^{\text{inf}}}{c_i^{\text{rhi}}}$, and $\frac{c_d^{\text{inf}}}{c_d^{\text{rhi}}}$.

As in Section 3.3, we assume the ratio of λ's is constant, and take it to equal the ratio of the v_{med}'s in Eq. (38). The functions $p(x)$, $f(x)$ and $g(x)$ and the constants N, V_{cone} and b are the same for influenza and rhinovirus. Moreover, the only difference between the two diseases in the random variables $D_r(j)$, $D_r(j)$ and $D_d(j)$ is the factor λ, which can be moved out of the integrals. Hence, conditioned on the values of the random variables that are common across the two diseases, we find that the ratio depends only on the α term times λ, i.e., $\frac{c_r^{\text{inf}}}{c_r^{\text{rhi}}} = \frac{\alpha_a^{\text{inf}}\lambda^{\text{inf}}}{\alpha_a^{\text{rhi}}\lambda^{\text{rhi}}} = 0.39$, $\frac{c_i^{\text{inf}}}{c_i^{\text{rhi}}} = \frac{\alpha_a^{\text{inf}}\lambda^{\text{inf}}}{\alpha_a^{\text{rhi}}\lambda^{\text{rhi}}} = 0.39$, and $\frac{c_d^{\text{inf}}}{c_d^{\text{rhi}}} = \frac{\alpha_n^{\text{inf}}\lambda^{\text{inf}}}{\alpha_n^{\text{rhi}}\lambda^{\text{rhi}}} = 7.6 \times 10^{-5}$, suggesting that—for an isolated sneeze or cough—relative to rhinovirus, influenza has greater contributions from respirable and inspirable transmission and less from droplet transmission.

5. Discussion

We begin our discussion with a comparison of our model and the Nicas–Sun model (2006), which to our knowledge is the first to present a mathematical model of the multiple modes of transmission. Although the framework (we use an infinite set of differential equations and they use a discrete-time Markov chain with 8 states) and presentation are somewhat different, there are remarkable similarities: both consider a model with aerosol transmission where deposition depends on particle size, and contact transmission with porous and nonporous surfaces (called textile and nontextile surfaces in Nicas and Sun, 2006), and both perform a separate analysis of droplet transmission from an isolated close expiratory event using a cone of infection emanating from a cough or sneeze. Our infection probability equation in (21) coincides with the inclusion-exclusion formula in Eq. (7) of Nicas and Sun if the shedding rate λ is deterministic (their inclusion-exclusion formula does not readily generalize to our random shedding case). The settings are somewhat different, in that we consider a four-person household model throughout the entire infectious period, whereas Nicas and Sun consider a health care worker and an infected during the symptomatic period. The main difference is probably the nature of the application of the models in the two papers: Nicas and Sun present a hypothetical but plausible example showing that a biocidal finish on textile surfaces has the potential to reduce contact transmission, whereas we focus in Section 3 on quantifying the routes of transmission for influenza (and in our companion paper Wein and Atkinson, 2006, on infection control measures related to face protection, ventilation and humidity) via the analysis of influenza and rhinovirus data.

We made several changes to our Section 4 after reading Section 5 of Nicas and Sun (2006). Our original analysis of a close expiratory event only considered droplet transmission, and assumed that virus (as opposed to virus-containing particles) was uniformly distributed within the cone, and ignored the stopping distance of particles. We made two

refinements to Section 4.3 that are contained in Section 5.1 of Nicas and Sun (2006): we assumed that particles (rather than virus) were uniformly distributed in the cone and considered the lower bound $\bar{d}$ of particles that would contribute to droplet transmission, which was derived by computing the stopping distances. Nicas and Sun also consider inspirable transmission in Section 5.2 of their paper, and so we added respirable and inspirable transmission from a close expiratory event in Sections 4.1 and 4.2 of our paper. In contrast to Section 5.2 of Nicas and Sun, we include a stopping distance analysis and assume that only the particles, and not both the particles and the virus, are uniformly distributed in the cone (indeed, inspired by Section 5.1 of Nicas and Sun) in Sections 4.1 and 4.2. Our stopping distance analysis suggests that respirable and inspirable transmission do not occur when the infected and susceptible are 60 cm apart (our original model allowed the distance to be uniformly distributed between 50 and 100 cm, but we changed it to 60 cm to enable easier comparison between our results and Nicas and Sun's).

We now turn to our results. The following picture emerges from our analysis of the household model. There is great interperson heterogeneity in viral shedding, and the majority of transmissions are caused by the largest shedders, which is reminiscent of superspreaders (Lloyd-Smith et al., 2005) (although our model does not capture the heterogeneity in infecteds' behavior); hence, the high correlation between viral shedding and symptoms suggests that our omission of asymptomatics is inconsequential. Most of the transmissions occur in a small time window near the time that symptoms appear, with just over half occurring during the presymptomatic period (slightly more than the 0.3–0.5 estimate in Fraser et al., 2004). The caregiver is approximately twice as likely to get infected as the noncaregiving susceptibles. A very small portion ($\approx 10^{-6}$) of the shed virus resides in particles that are small enough to be airborne; it is the larger (>3 μm) droplet nuclei that inflict most of the damage because they make up most of the deposition in the respiratory epithelium, which is the location of infection in our model. Nonetheless, influenza virus dies much more quickly on the hands than in the air, and much more virus is required for contact or droplet infection than an aerosol infection, and taken together, aerosol transmission is far more dominant than contact transmission. However, nearly all of the aerosol transmission is within-room because of the high settling rate of the >3 μm droplet nuclei.

Our main finding about the dominance of aerosol transmission over contact transmission for influenza is highly suggestive, but not definitive. The main caveat is that our analysis is based on interpandemic influenza strains, and the characteristics (Table 2) of a future pandemic influenza strain cannot be accurately predicted. However, there are at least several orders-of-magnitude slack behind this finding, and hence several of our parameter values would have to be highly inaccurate—and biased toward aerosol transmission—to negate it. The 1918 influenza (Tumpey et al., 2005), the 1957 pandemic strain (Hers and Mulder, 1961) and the current H5N1 virus (Shinya et al., 2006) all appear to target the alveolar region in addition to the interpandemic target of the respiratory epithelium, which would strengthen the importance of aerosol transmission if it was included in our model. While our model contains many simplifying and detailed assumptions so that we could quantify the routes of transmission in a household throughout the entire infectious period, to assess the robustness of our conclusions we now change the values of the parameters (in the interpandemic setting) that we suspect may impact the results. Although the fraction of infections due to contact transmission is sensitive to the self-inoculation rate and the death rate of the virus on hands, we conservatively used a

self-inoculation rate that is 6 times higher than that measured without others observing them (Hendley et al., 1973). If we decrease the death rate on the hands, μ_h, to 10/hour (which is a factor of 5 less than the value we use in our model, which itself is the more conservative value from Bean et al., 1982) the fraction of infections via contact transmission increases to 0.21. One of the reasons for the dominance of aerosol transmission is the huge discrepancy between the values of ID_{50}^a and ID_{50}^n, which were derived using different influenza A strains and different assay procedures. If we increase ID_{50}^a by a factor of 100 to 67.1 $TCID_{50}$, the fraction of infections via contact transmission increases to only 0.006. Also, a key parameter that governs the amount of contact transmission is the composite surface contact parameter ϕ. Assuming no virus transfer and no handwashing, both of which increase contact transmission, a sensitivity analysis shows that ϕ would need to be 6.6×10^4 higher in the symptomatic period than the presymptomatic period to increase the fraction of infections that are via contact transmission to 0.1. Although this increase seems impractically high, we have treated ϕ as a constant in our model, whereas it likely varies significantly for each pair of persons. Hence, we cannot dismiss the possibility of occasional contact transmission in certain circumstances (e.g., mother-infant interaction).

Droplet transmission, which is the third mode of transmission in much of the literature, is difficult to analyze directly without reliable data on how often people are in close (<1 m) contact, their relative heights and the directions of emitted sneezes and coughs. In Section 4, we analyze a geometric model of a close (60 cm) expiratory event, which allows for respirable transmission (immediate inhalation of <20 μm particles), inspirable transmission (immediate inhalation of [20, 200] μm particles) and droplet transmission (direct deposition of large particles on the mucous membrane). If we ignore the theoretical stopping distances of respirable and inspirable particles, then the infection probability for a cough is 0.244, with nearly 90% of the contribution coming from inspirable transmission, and the infection probability of a sneeze is 0.9999 with all three routes of transmission being potent. If we more realistically incorporate the stopping distances of respirable and inspirable particles, then the infection probability—all due to droplet transmission—is 0.011 for a cough and 0.981 for a sneeze.

Several behavioral and physical factors suggest that actual transmission during close expiratory events may be considerably less than predicted in Section 4. Sneezes, and to a lesser extent coughs, are typically directed at a downward angle, and both are usually protected when two people are within 60 cm of each other. Furthermore, nasal openings are also oriented downward (in contrast, the simple analysis in this section assumes nostrils are more like a pig's snout), making it difficult for droplets to land inside a susceptible's nose unless the infected is at a lower height than the susceptible and the sneeze or cough is directed upwards. Also, we assume that the particles are uniformly distributed in this cone, but most of the virus may be concentrated close to the center of the cone. Nonetheless, during the symptomatic period, infecteds may be too weak to protect their sneezes and coughs and may, while bedridden, be at a lower height than the susceptible. Also, as noted above, some of our calculations in Section 4 assume that all <200 μm particles are uniformly distributed in the cone that the susceptible inhales from, whereas the largest inspirable particles only travel 6 inches from the infected during a cough. It is also interesting to note that droplet transmission was never considered a significant factor in rhinovirus transmission by the two research groups who studied it deeply: the Wisconsin group argued that there was a large aerosol component (Jennings and Dick, 1987) and the Virginia group argued that there was a significant contact component (Hendley

and Gwaltney, 1988). While it is possible that both groups headed down the wrong track (e.g., because droplet transmission was to difficult to study experimentally), it does not seem likely. Suppose for the moment that they were wrong, and that droplet transmission and aerosol transmission made equal contributions to rhinovirus transmission. That is, combining all 5 routes of transmission together, if we are given the doses from each type of transmission, then our probability of infection is $P_I = 1 - e^{-(c_a+c_s+c_r+c_i+c_d)}$, and we are setting $c_a^{\text{rhi}} = c_d^{\text{rhi}}$ (our reanalyses in Appendices A and B reinforce the belief that aerosol transmission for rhinovirus is significant). Then assuming the ratios computed in Section 4.5 for one cough or sneeze are valid for multiple ones over an entire infectious period, our computed ratios imply that $c_d^{\text{inf}} = 9.9 \times 10^{-5} c_a^{\text{inf}}$, i.e., the contribution from droplet transmission in influenza is trivial relative to aerosol transmission.

We now review our main finding about the primacy of the aerosol route of transmission with respect to the literature (recently reviewed in Tellier, 2006), starting with the 1977 airplane outbreak (Moser et al., 1979). We estimate the viral shedding rate from this outbreak and compare it to our estimate of the median initial shedding rate e^{m_λ} from Section 3.5. We assume all transmission is via aerosol and use all of our relevant parameters in Table 1 except we let $V = 168$ m^3 (Moser et al., 1979; Rudnick and Milton, 2003), $\frac{Q}{V} = 0.1$/hr (Moser et al., 1979; Rudnick and Milton, 2003), and $T = 4.5$ hr, and let λ denote the constant unknown viral shedding rate. Of the 29 susceptibles who stayed on board for the entire 4.5 hr, 25 of them were infected. We equate the probability of aerosol infection, $1 - e^{-\alpha_a \bar{D}_a}$, to $\frac{25}{29}$, and solve for λ, where $\bar{D}_a = \int_0^{d_c} D_a(x) g(x)\, dx$ and $D_a(x)$ is given in Eq. (30), and find that the shedding rate was $\lambda = 8.53 \times 10^{10}$ TCID$_{50}$/day. If the infected person on the airplane was at her peak shedding rate, then her initial shedding rate was $e^{-4.94}(1.84 \times 10^{10}) = 6.11 \times 10^8$ TCID$_{50}$/day. Assuming log-normal initial viral shedding rates with $e^{m_\lambda} = 2.88 \times 10^7$ TCID$_{50}$/day (from Section 3.5) and $e^{\sigma_\lambda} = 40$, the infected's value of 6.11×10^8 TCID$_{50}$/day is at the 0.80 fractile. That is, the infected on the airplane was a higher-than-typical shedding rate, but was not a statistical outlier.

Our main finding is also consistent with a 1957–1958 observational study in a hospital that compared two wards, one of which had ultraviolet light radiation and many fewer influenza cases (McLean, 1961). Very few interroom aerosol transmissions occur in our model, which is consistent with experience in hospitals (Bridges et al., 2003). Our claim is also consistent with the observation that intranasal antivirals are effective in experimental intranasal infections of influenza (Calfee et al., 1999) but ineffective against natural influenza (Tannock et al., 1988; Kaiser et al., 2000), whereas inhaled antivirals are effective against natural influenza (Kaiser et al., 2000; Hayden et al., 2000). The importance of aerosol transmission for influenza appears to have been an accepted notion in the 1970s (Douglas, 1975; Knight, 1973; Fox and Kilbourne, 1973), which was an active period of research during which human volunteer studies were possible. Our results are also not inconsistent with a large ($>10^6$ person-weeks of data) military study of handwashing, which found a significant reduction in total illness (i.e., 45% reduction in outpatient visits for respiratory illness) without a statistically significant reduction in hospitalizations or severe illness (Ryan et al., 2001), raising the possibility that handwashing is more effective against less virulent rhinoviruses than against influenza. Finally, our claim is inconsistent with nurse-to-patient direct contact transmissions during tube feeding and suctioning in hospitals (Morens and Rash, 1995), although these procedures are not typically undertaken in the home.

Our analysis raises several open questions. One inconsistency arose during our model calibration: for both rhinovirus and influenza, an independent estimate of the median viral shedding rate e^{m_λ}, which was based on first principles and 7 primitive parameters that are difficult to estimate (volume per droplet, number of droplets in a cough and sneeze, virus concentration in a cough and sneeze, and sneezing and coughing rates), was 1–4 orders-of-magnitude smaller than the estimate used in this study, which was backed out of our model from the observed proportion of people infected. The underlying reason for this discrepancy remains unclear, although we do not believe the model itself has omitted or misrepresented any factors that could cause a difference of this magnitude. One possible reason is that the health status of the subjects in existing studies on the number of droplets in a sneeze or cough is unknown, although they were likely to be healthy (Nicas et al., 2005), which would cause the first-principles approach to generate an underestimate because infected people excrete more nasal discharge and sputum than healthy people. A related question is the relative importance for aerosol transmission of sneezing vs. coughing: while sneezing discharge rates appear to be several orders-of-magnitude higher than coughing discharge rates, the health status of the subjects in existing studies are unknown (Nicas et al., 2005), cough particles may be smaller than sneeze particles (Fox and Kilbourne, 1973; Winkler, 1973) despite data that we use suggesting they have the same size distribution (Duguid, 1946), rhinovirus data suggest that coughing rates may be a better predictor of transmission than sneezing rates (Appendix B), unprotected droplet nuclei <20 μm in diameter may be more apt to be deposited on surfaces if they are from sneezes rather than coughs because of the downward orientation of most sneezes, and the infected in the 1977 influenza outbreak on an airplane was noted to be coughing but there was no mention of sneezing (Moser et al., 1979). Finally, if droplet transmission is an important contributor to rhinovirus infection, then people who wear eyeglasses should catch the common cold less frequently than other people (because of the difficulty of droplet transmission through the mouth or nose). This would appear to be a testable hypothesis. In any case, the issues raised in this paragraph largely disappear when one computes the ratios $\frac{c_a^{\text{inf}}}{c_a^{\text{rhi}}}$, $\frac{c_s^{\text{inf}}}{c_s^{\text{rhi}}}$ and $\frac{c_d^{\text{inf}}}{c_d^{\text{rhi}}}$, and hence the core of our argument remains intact.

In conclusion, our analysis suggests that aerosol transmission (inhaling <20 μm droplet nuclei that reside in the air) is far more dominant than contact transmission for influenza. The likelihood of droplet transmission from a close unprotected cough appears to be quite small, but a close unprotected horizontally-directed face-to-face sneeze is potent enough to cause droplet transmission. Although such events seem rare among adults, insufficient data exist on their frequency, and droplet transmission for influenza cannot be dismissed without future empirical investigation.

Acknowledgements

L.M.W. was partially supported by the Center for Social Innovation, Graduate School of Business, Stanford University, and M.P.A. was supported by an Abbott Laboratories Stanford Graduate Fellowship. L.M.W. thanks Richard Danzig for suggesting this problem to him.

Appendix A: Airborne rhinovirus experiments

In Dick et al. (1987), 10 of 18 susceptibles (5/6, 1/6 and 4/6 in experiments A, B and C) who were physically restricted from touching their hands to their face became infected after playing cards for 12 hours with 8 infected people in a room of size $V = 92.5$ m^3. Infecteds in these experiments were cycled in and out of the room so that all infecteds in the room had severe colds. Table 1 of Dick et al. (1987) states the geometric mean and maximum viral nasal concentration in each of the 3 experiments, along with the total number of coughs, sneezes and nose blows (and range across individual infecteds), where the means and maximums are of the 8 infecteds among approximately 30 that had the most severe symptoms (and hence were chosen to play cards with the susceptibles).

Our primary goal in this subsection is to estimate e^{m_λ} from the data in Dick et al. (1987). Because the data are aggregated so that we do not know the number of sneezes and coughs and the nasal concentration of each infected individual, we indirectly estimate e^{σ_λ}. The median (over the 3 experiments) nasal concentration is 1.9×10^5 TCID$_{50}$/mL, after accounting for 10 mL of nasal wash, which is very similar to the geometric mean of the 3 geometric means, which is 1.7×10^5 TCID$_{50}$/mL. The median maximum concentration is 10^6 TCID$_{50}$/mL. Letting $G(x)$ be the log-normal cdf with median 1.9×10^5 TCID$_{50}$/mL and dispersal factor e^{σ_x}, we solve for σ_x such that the median of the maximum of the nasal concentrations of the 8 infecteds, $\max(X_1, \ldots, X_8)$, equals 10^7 TCID$_{50}$/mL (i.e., $G(10^7)^8 = 0.5$), to get $e^{\sigma_X} = 17.3$. To estimate e^{σ_Y}, we first note that the mean coughing plus sneezing rate is 7.32/hr (we ignore nose-blowing). If we let $Y_1, \ldots, Y_8$ be the sneezing plus coughing rate for the 8 infecteds, then the median (over the 3 experiments) maximum divided by the median minimum is $\frac{\text{med}[\max(Y_1,\ldots,Y_8)]}{\text{med}[\min(Y_1,\ldots,Y_8)]} = \frac{282}{9} = 31.3$. Solving for e^{σ_Y} given a mean of 7.32 and the ratio of 31.3 gives $e^{\sigma_Y} = 3.5$. The quantities $e^{\sigma_X} = 17.3$ and $e^{\sigma_Y} = 3.5$ generate $e^{\sigma_\lambda} = 22.5$ and 60.5 for the independent and perfectly-correlated cases, respectively. We set $e^{\sigma_\lambda} = 50$, which corresponds to $\rho = 0.79$.

We solve $1 - \int_0^\infty e^{-\alpha_a \bar{D}_a(\lambda)} h(\lambda)\, d\lambda = \frac{10}{18}$ for e^{m_λ}, where $\bar{D}_a = \int_0^{d_c} D_a(x) g(x)\, dx$, $D_a(x)$ is given in Eq. (30), $h(\lambda)$ is the $(e^{m_\lambda}, e^{\sigma_\lambda})$ log-normal pdf, and for lack of data $\frac{Q}{V} = 1.0$/hr. This yields $e^{m_\lambda} = 1.19 \times 10^9$ TCID$_{50}$/day, after dividing by 8, which is the number of infecteds in the room.

We can also attempt to estimate the median shedding rate e^{m_λ} for this experiment from first principles. Assuming that throat concentrations are a factor of ten less than nasal concentrations (Hendley and Gwaltney, 1988), we find that the median total shedding rate is 8.07×10^7 TCID$_{50}$/day, which is the sum of the contribution from sneezes,

$$\begin{aligned}
&\left(1.7 \times 10^5 \frac{\text{TCID}_{50}}{\text{mL}}\right)\left(0.45 \frac{\text{sneezes}}{\text{person} \cdot \text{hr}}\right)\left(8 \text{ people}\right)\left(24 \frac{\text{hr}}{\text{day}}\right) \\
&\quad \times \left(9.4 \times 10^4 \frac{\text{droplets}}{\text{sneeze}}\right)\left(5.733 \times 10^7 \frac{\mu\text{m}^3}{\text{droplet}}\right)\left(\frac{\text{mL}}{(10^4)^3 \mu\text{m}^3}\right) \\
&\quad = 8.01 \times 10^7 \frac{\text{TCID}_{50}}{\text{day}}, \qquad \text{(A.1)}
\end{aligned}$$

and the contribution from coughs,

$$\left(1.7 \times 10^4 \frac{\text{TCID}_{50}}{\text{mL}}\right)\left(6.87 \frac{\text{coughs}}{\text{person} \cdot \text{hr}}\right)\left(8 \text{ people}\right)\left(24 \frac{\text{hr}}{\text{day}}\right)$$
$$\times \left(470 \frac{\text{droplets}}{\text{cough}}\right)\left(5.733 \times 10^7 \frac{\mu\text{m}^3}{\text{droplet}}\right)\left(\frac{\text{mL}}{(10^4)^3 \mu\text{m}^3}\right)$$
$$= 6.1 \times 10^5 \frac{\text{TCID}_{50}}{\text{day}}, \tag{A.2}$$

where the mean volume is calculated using the truncated mixture of log-normals. Dividing this quantity by the 8 people gives a shedding rate of 1.01×10^7 TCID_{50}/day, which is 112 times smaller than the estimate of e^{m_λ} from solving $1 - \int_0^\infty e^{-\alpha_a \bar{D}_a(\lambda)} h(\lambda)\, d\lambda = \frac{10}{18}$. We suspect that much of this difference is due to the likelihood that the droplets per sneeze and cough in (A.1), (A.2) are based on healthy individuals who shed fewer particles per cough and sneeze than if they were infected; indeed, had we used the estimate of 5000 droplets per cough (Duguid, 1946) (likely also from healthy subjects) rather than 470, the two shedding estimates would be off by a factor of 10.5 rather than 112. In addition, the 2.95×10^6 TCID_{50}/day estimate excludes viral shedding from nose blows.

An interesting observation is that the experiment (experiment B) with the highest nasal concentration and the largest number of sneezes led to the least number of airborne infections ($\frac{1}{6}$). However, experiment B had the least number of coughs, raising the possibility that although sneezes contain much more virus than coughs (Eqs. (A.1), (A.2) suggest that approximately 99% of the shed virus is in sneezes), it is actually the coughs that cause most of the airborne infections. If this observation is not simply due to chance (which is possible given the small number of susceptibles involved), a possible reason for this is that nearly all of the virus shed from a sneeze settles on a surface (in these experiments, susceptibles and infecteds were sitting around tables playing cards) because of the large velocity and natural downward trajectory of a sneeze; in contrast, a cough typically has a smaller velocity and an outward trajectory. A related observation is that the authors of Moser et al. (1979) note that the infected in the 1977 airplane outbreak (see Section 5) coughed, but say nothing about the infected sneezing.

Although it is less informative, we analyze the other rhinovirus experiment that disallowed contact transmission, which is the small-particle aerosol exposure in Gwaltney et al. (1978). It took place for 72 continuous hours in a large, closed room (the size of two hotel rooms, personal communication, Jack Gwaltney) with one infected and with continuous airflow but no fresh air introduced. For lack of data, we assume a $\frac{Q}{V}$ ratio of 1.0/hr and let $V = 250$ m^3. We assume the infected had a median viral nasal concentration of $5 \times 10^{1.5}$ TCID_{50}/mL (Gwaltney et al., 1978), a median viral throat concentration of $10^{1.2}$ (this is the concentration in saliva, which is typically similar to the concentration in the throat Hendley et al., 1973, Hendley and Gwaltney, 1988), sneezed at a constant rate of 3/day (Gwaltney et al., 1978), and coughed at a constant rate of 70/day (Gwaltney et al., 1978), yielding a median viral shedding rate of $e^{m_\lambda} = 2585.9$ TCID_{50}/day. We set the dispersion $e^{\sigma_X} = 5$ for nasal concentration because the variability appears to be considerably less than in Dick et al. (1987). We set $e^{\sigma_\lambda} = 15$, which corresponds to $\rho = 0.79$ with $e^{\sigma_Y} = 3.5$ derived earlier from Dick et al. (1987). Zero of 10 people were infected in this experiment. This yields $p_I = 1.90 \times 10^{-5}$, which implies that the probability of

0/10 infected is 0.9998. If we assume that the first-principles estimate of e^{m_λ} is underestimated by the factor 112 as in our analysis of the study in Dick et al. (1987), then $p_I = 1.76 \times 10^{-3}$ and the probability of 0/10 infected is 0.9825. In either case, we would have expected the 0/10 outcome.

Appendix B: Rhinovirus experiments with all modes transmission

The six rhinovirus experiments (labeled A–F) in Meschievitz et al. (1984) allow for aerosol transmission, contact transmission and droplet transmission, and report the fraction infected for various amounts of infected hours of exposure (referred to as donor hours of exposure in Meschievitz et al., 1984) in a closed room of volume $V = 186.4$ m^3 (experiment A has $V = 84.6$ m^3) with recirculating air conditioning. If we let T equal infected hours of exposure and assume that the viral shedding rate is not random, then our analysis (see Eqs. (31) and (36)) predicts that $P_I = 1 - e^{-cT}$ for some constant c that may include contributions from all three modes of transmission. This equation provides a good fit to the data with $c = 0.0043$/infected-hr (Fig. B.1a) for experiments B–F; experiment A, which has a different room volume, will be analyzed shortly.

Table 3 of Meschievitz et al. (1984) provides additional information about the experiments, including the geometric mean of virus nasal concentration, mean symptom score of infecteds (both means are for the ≈7 among ≈22 infecteds that had the most severe symptoms and were consequently chosen as donors), and the fraction of infected hours during waking hours. However, the fractions infected in experiments B–F of Meschievitz et al. (1984) appear to depend solely on the infected-hours of exposure and to be largely independent of the geometric mean shedding rates and the mean symptom scores (e.g., experiment C has a much smaller geometric mean shedding rate than the other four experiments with $V = 186.4$ m^3). This independence is not necessarily inconsistent with our model, which predicts (see Section 3.5) that most transmission is caused by the highest-shedding infecteds (as this Wisconsin research group found in D'Alessio et al., 1976). That is, our model would be consistent with the data in Meschievitz et al. (1984) if the shedding rates of the highest shedders were similar across experiments. Although Meschievitz et al. (1984) contains insufficient data (we would need the virus concentration and the sneezing and coughing rates of each donor) to verify whether this is true, extreme-value theory (Leadbetter et al., 1980) applied to the maximum of 22 log-normal random variables with median and dispersal factor derived from the data in Dick et al. (1987) implies that the maximum shedding rate among all 22 infecteds has considerable variability (i.e., the standard deviation is larger than the mean).

Two other observations (not pointed out in Meschievitz et al., 1984 or Dick et al., 1987) suggest that perhaps a nontrivial fraction of infection transmissions in these experiments is airborne. First, the fraction of infected-hours in which infecteds are asleep (and presumably during which contact transmission cannot occur) varies between 0.14 (experiment D) and 0.30 (experiment E) in these experiments, and yet appears to have no impact on the transmission probability. Second, leaving aside the possible differences in e^{m_λ} in Meschievitz et al. (1984) and Dick et al. (1987) (both used the same inoculation method and similar pool-sizes of infecteds), the only difference between these two sets of experiments in terms of our airborne model in Eq. (31) is the room volume V. Hence, if

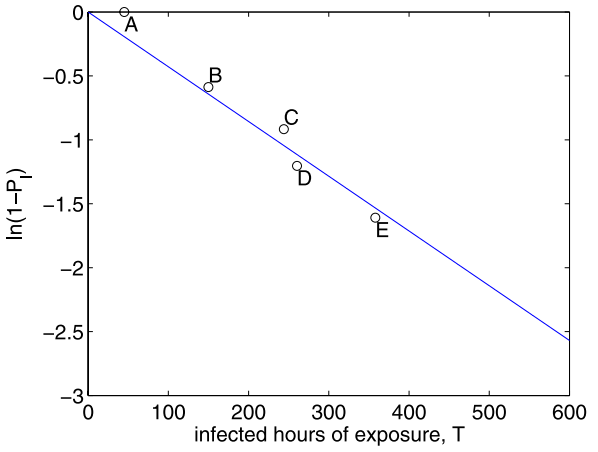

(a)

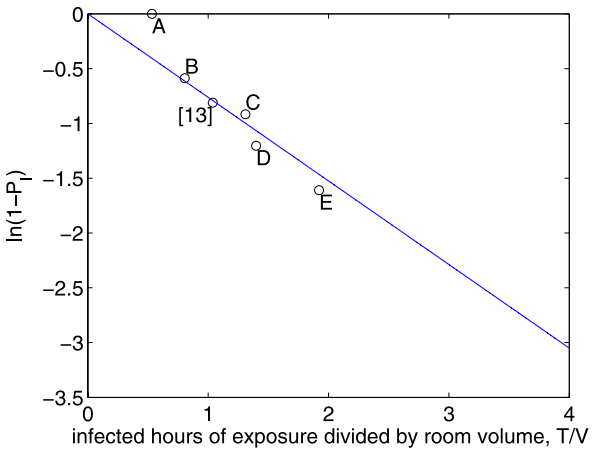

(b)

Fig. B.1 Rhinovirus experiments. (a) Fitting data from the all-modes-of-transmission experiments B–E in Meschievitz et al. (1984) on the fraction infected vs. infected hours of exposure (T) using the equation $P_I = 1 - e^{-cT}$, which assumes that the viral shedding rate is a constant, yields $c = 0.0043$/infected-hr. Experiment F of Meschievitz et al. (1984) had $T = 585$ and resulted in all five people getting infected, which we predict would occur with probability $(1 - e^{-2.5})^5 = 0.66$. (b) Fitting data from experiments A–E in Meschievitz et al. (1984) and the airborne experiments in Dick et al. (1987) using the aerosol transmission equation $P_I = 1 - e^{-\frac{cT}{V}}$, where V is room volume and the viral shedding rate is a constant, yields $c = 0.7625$ m^3/infected-hr.

transmission is via aerosol, then we predict that $p_I = 1 - e^{-\frac{cT}{V}}$, where c is interpreted differently than the earlier constants. Fitting the experiments from Meschievitz et al. (1984) and Dick et al. (1987) (including experiment A from Meschievitz et al., 1984) to this refined model still yields an excellent fit to six of the seven experiments with $c = 0.7625$ m^3/infected-hr (Fig. B.1b). In particular, the fact that the airborne transmission experi-

ments in Dick et al. (1987) coincide with the all-modes-of-transmission experiments in Meschievitz et al. (1984), after accounting for room volume, raises the possibility that nearly all transmissions in Meschievitz et al. (1984) were from aerosol. Experiment A is the only experiment that does not fall close to our predicted curve: the probability of 0/5 infected according to our model is $(e^{-0.406})^5 = 0.13$ (with the small number of subjects involved, the likelihood of a good fit for all seven experiments is small). However, this experiment had by far the smallest geometric mean shedding rate among the six experiments in Meschievitz et al. (1984) and its maximum nasal virus concentration was smaller than the geometric mean concentrations for all other experiments except for C, and hence the results of this experiment are not inconsistent with a more refined model of the form $p_I = 1 - e^{-\frac{c\lambda T}{V}}$.

Because the airborne experiments in Dick et al. (1987) fit the model for the experiments in Meschievitz et al. (1984), it is difficult to obtain additional information from the data in Meschievitz et al. (1984). For example, if we assume that the values $e^{m_\lambda} = 1.19 \times 10^9$ TCID_{50}/day and $e^{\sigma_\lambda} = 50$ derived from the experiments in Dick et al. (1987) also hold for Meschievitz et al. (1984) (the experiments in Meschievitz et al., 1984 and Dick et al., 1987 had similar inoculation methods and comparable donor pools, with 8 of 30 donors used in Dick et al., 1987 vs. 7 out of 22 in Meschievitz et al., 1984), and we estimate ϕ by minimizing the sum over the six experiments in Meschievitz et al. (1984) of the squared difference of $1 - \int_0^\infty e^{-(\alpha_a \bar{D}_a(\lambda) + \alpha_n \bar{D}_s(\lambda))} h(\lambda)\, d\lambda$ and the actual fraction infected, then we predict that there is essentially no contact transmission (i.e., $\phi \approx 0$ $\frac{\text{m}^2}{\text{hr}}$, details not shown). Similarly, if we assume all transmissions are aerosol and a log-normal virus shedding rate with $e^{\sigma_\lambda} = 50$ as in Appendix A, and we estimate e^{m_λ} by minimizing the sum of squares over the six experiments in Meschievitz et al. (1984) (each with a different value of T) of $\int_0^\infty e^{-\alpha_a \bar{D}_a(\lambda)} h(\lambda)\, d\lambda$ minus the actual fraction infected, then we get an estimate of $e^{m_\lambda} = 1.63 \times 10^9$ TCID_{50}/day (details not shown), which is very similar to the estimate based on data in Dick et al. (1987).

The data in Meschievitz et al. (1984) offers an alternative rough estimate of e^{m_λ}. We first take a weighted average of the 16 geometric mean concentrations in Table 3 of Meschievitz et al. (1984), where the weights are the fractions of donor-hours of exposure, and get 2.42×10^4 TCID_{50}/mL. Following the procedure used in Eqs. (A.1), (A.2) for sneezes and coughs (because Meschievitz et al., 1984 contains no cough and sneeze data, we estimate these rates by deriving the ratio of mean symptom scores from Meschievitz et al., 1984 and Dick et al., 1987, and then multiply this ratio times the cough and sneeze rates in Dick et al., 1987),

$$\begin{aligned}
&\left(2.42 \times 10^4 \frac{\text{TCID}_{50}}{\text{mL}}\right)\left(0.35 \frac{\text{sneezes}}{\text{person} \cdot \text{hr}}\right)\left(24 \frac{\text{hr}}{\text{day}}\right)\left(9.4 \times 10^4 \frac{\text{droplets}}{\text{sneeze}}\right) \\
&\quad \times \left(5.733 \times 10^7 \frac{\mu\text{m}^3}{\text{droplet}}\right)\left(\frac{\text{mL}}{(10^4)^3 \mu\text{m}^3}\right) \\
&\quad = 1.10 \times 10^6 \frac{\text{TCID}_{50}}{\text{day}}, \qquad \text{(B.1)}
\end{aligned}$$

and

$$\left(2.42 \times 10^3 \frac{\text{TCID}_{50}}{\text{mL}}\right)\left(5.3 \frac{\text{coughs}}{\text{person} \cdot \text{hr}}\right)\left(24 \frac{\text{hr}}{\text{day}}\right)\left(470 \frac{\text{droplets}}{\text{cough}}\right)$$
$$\times \left(5.733 \times 10^7 \frac{\mu\text{m}^3}{\text{droplet}}\right)\left(\frac{\text{mL}}{(10^4)^3 \mu\text{m}^3}\right)$$
$$= 8.3 \times 10^3 \frac{\text{TCID}_{50}}{\text{day}}, \tag{B.2}$$

we get $e^{m_\lambda} = 1.10 \times 10^6$ TCID_{50}/day, which is 1.08×10^3 times smaller than our estimate from Dick et al. (1987).

References

Alford, R.H., Kasel, J.A., Gerone, P.J., Knight, V., 1966. Human influenza resulting from aerosol inhalation. Proc. Soc. Exp. Biol. Med. 122, 800–804.

Ansari, S.A., Springthorpe, V.S., Sattar, S.A., Rivard, S., Rahman, M., 1991. Potential role of hands in the spread of respiratory viral infections: studies with human parainfluenza virus 3 and rhinovirus 14. J. Clin. Mircobiol. 29, 2115–2119.

Ball, F., Neal, P., 2002. A general model for stochastic SIR epidemics with two levels of mixing. Math. Biosci. 180, 73–102.

Barry, J.M., 2004. The Great Influenza. Penguin Books, London.

Bean, B., Moore, B.M., Sterner, B., Peterson, L.R., Gerding, D.N., Balfour, H.H. Jr., 1982. Survival of influenza virus on environmental surfaces. J. Infect. Dis. 146, 47–51.

Bridges, C.B., Kuehnert, M.J., Hall, C.B., 2003. Transmission of influenza: implications for control in health care settings. Clin. Infect. Dis. 37, 1094–1101.

Bynoe, M.L., Hobson, D., Horner, J., Kipps, A., Schild, G.C., Tyrrell, D.A.J., 1961. Inoculation of human volunteers with a strain of virus isolated from a common cold. Lancet 1, 1194–1196.

Calfee, D.P., Peng, A.W., Hussey, E.K., Lobo, M., Hayden, F.G., 1999. Safety and efficacy of once daily intranasal zanamivir in preventing experimental human influenza A infection. Antivir. Ther. 4, 143–149.

Carrat, F., Sahler, C., Rogez, S., Leruez-Ville, M., Freymuth, F., Le Gales, C., Bungener, M., Houseet, B., Nicolas, M., Rouzioux, C., 2002. Influenza burden of illness. Arch. Intern. Med. 162, 1842–1848.

Cate, T.R., Couch, R.B., Johnson, K.M., 1964. Studies with rhinoviruses in volunteers: production of illness, effect of naturally acquired antibody, and demonstration of a protective effect not associated with serum antibody. J. Clin. Investig. 43, 56–67.

Cauchemez, S., Carrat, F., Viboud, C., Valleron, A.J., Boelle, P.Y., 2004. A Bayesian MCMC approach to study transmission of influenza: application to household longitudinal data. Stat. Med. 23, 3469–3487.

Committee on the Development of Reusable Facemasks for Use During an Influenza Pandemic, Institute of Medicine, 2006. Reusability of Facemasks During an Influenza Pandemic. National Academies Press, Washington.

Connor, R.J., Kawaoka, Y., Webster, R.G., Paulson, J.C., 1994. Receptor specificity in human, avian, and equine H2 and H3 influenza virus isolates. Virology 203, 17–23.

Couch, R.B., Gerone, P.J., Cate, T.R., Griffith, W.R., Alling, D.W., Knight, V., 1965. Preparation and properties of a small-particle aerosol of coxsackie A21. Proc. Soc. Exp. Biol. Med. 118, 818.

Couch, R.B., Cate, T.R., Douglas, R.G. Jr., Gerone, P.J., Knight, V., 1966. Effect of route of inoculation on experimental respiratory viral disease in volunteers and evidence for airborne transmission. Bacteriol. Rev. 30, 517–529.

Couch, R.B., Douglas, R.G. Jr., Fedson, D.S., Kasel, J.A., 1971. Correlated studies of a recombinant influenza-virus vaccine. III. Protection against experimental influenza in man. J. Infect. Dis. 124, 473–480.

Couch, R.B., Kasel, J.A., Gerin, J.A., Schulman, J.L., Kilbourne, E.D., 1974. Induction of partial immunity to influenza by a neuraminidase-specific vaccine. J. Infect. Dis. 129, 411–420.

D'Alessio, D.J., Peterson, J.A., Dick, C.R., Dick, E.C., 1976. Transmission of experimental rhinovirus colds in volunteer married couples. J. Infect. Dis. 133, 28–36.
D'Alessio, D.J., Meschievitz, C.K., Peterson, J.A., Dick, C.R., Dick, E.C., 1984. Short-duration exposure and the transmission of rhinoviral colds. J. Infect. Dis. 150, 189–194.
de Jong, M.D., Tran, T.T., Truong, H.K., Vo, M.H., Smith, G.J., Chau, N.V., Van Cam, B., Qui, P.T., Ha, D.Q., Guan, Y., Peiris, J.S.M., Hien, T.T., Farrar, J., 2005. Oseltamivir resistance during treatment of infleunza A (H5N1) infection. N. Engl. J. Med. 353, 2667–2672.
Dick, E.C., Jennings, L.C., Mink, K.A., Wartgow, C.D., Inhorn, S.L., 1987. Aerosol transmission of rhinovirus colds. J. Infect. Dis. 156, 442–448.
Douglas, R.G., 1970. Pathogenesis of rhinovirus common colds in human volunteers. Ann. Otol. Rhinol. Laryngol. 79, 563–571.
Douglas, R.G. Jr., 1975. Influenza in man. In: Kilbourne, E.D. (Ed.), The Influenza Viruses and Influenza, pp. 395–447. Academic Press, New York.
Douglas, R.G. Jr., Cate, T.R., Gerone, P.J., Couch, R.B., 1966. Quantitative rhinovirus shedding patterns in volunteers. Am. Rev. Respir. Dis. 94, 159–167.
Duguid, J.P., 1946. The size and duration of air-carriage of respiratory droplets and aerosol. J. Hyg. 4, 471–480.
Ferguson, N., Cummings, D.A.T., Cauchemez, S., Fraser, C., Riley, S., Meeyai, A., Iamsirithaworn, S., Burke, D.S., 2005. Strategies for containing an emerging influenza pandemic in Southeast Asia. Nature 437, 209–214.
Fox, J.P., Kilbourne, E.D., 1973. From the National Institutes of Health: epidemiology of influenza—summary of influenza workshop IV. J. Infect. Dis. 128, 361–386.
Fox, J.P., Cooney, M.K., Hall, C.E., 1975. The Seattle virus watch. Am. J. Epidemiol. 101, 122–143.
Fox, J.P., Cooney, M.K., Hall, C.E., Foy, H.M., 1985. Rhinoviruses in Seattle families, 1975–1979. Am. J. Epidemiol. 122, 830–846.
Fraser, C., Riley, S., Anderson, R.M., Ferguson, N.M., 2004. Factors that make an infectious disease outbreak controllable. PNAS 101, 6146–6151.
Gerone, P.J., Couch, R.B., Keefer, G.V., Douglas, R.G., Derrenbacker, E.B., Knight, V., 1966. Assessment of experimental and natural viral aerosols. Bact. Rev. 30, 576.
Gwaltney, J.M. Jr., Moskalski, P.B., Hendley, J.O., 1978. Hand-to-hand transmission of rhinovirus colds. Ann. Intern. Med. 88, 463–467.
Hall, C.B., Douglas, R.G. Jr., Geiman, J.M., Meagher, M.P., 1979. Viral shedding patterns of children with influenza B infection. J. Infect. Dis. 140, 610–613.
Harper, G.J., 1961. Airborne micro-organisms: survival tests with four viruses. J. Hyg. (Camb.) 59, 479–486.
Hayden, F.G., Treanor, J.J., Betts, R.F., Lobo, M., Esinhart, J.D., Hussey, E.K., 1996. Safety and efficacy of the neuraminidase inhibitor GG167 in experimental human influenza. JAMA 275, 295–299.
Hayden, F.G., Fritz, R.S., Lobo, M.C., Alvord, W.G., Strober, W., Straus, S.E., 1998. Local and systemic cytokine responses during experimental human influenza A virus infection. J. Clin. Inv. 101, 643–649.
Hayden, F.G., Gubareva, L.V., Monto, A.S., Klein, T.C., Elliott, M.J., Hammond, J.M., Sharp, S.J., Ossi, M.J., 2000. Inhaled zanamivir for the prevention of influenza in families. NEJM 343, 1282–1289.
Health and Human Services Department, U.S. Government, 2004. HHS Pandemic Influenza Plan. Health and Human Services Department, Washington.
Heinsohn, R.J., Cimbala, J.M., 1999. Indoor Air Quality Engineering. Dekker, New York.
Hemmes, J.H., Winkler, K.C., Kool, S.M., 1960. Virus survival as a seasonal factor in influenza and poliomyelitis. Nature 188, 430–431.
Hendley, J.O., Wenzel, R.P., Gwaltney, J.M. Jr., 1973. Transmission of rhinovirus colds by self-inoculation. NEJM 288, 1361–1364.
Hendley, J.O., Gwaltney, J.M. Jr., 1988. Mechanisms of transmission of rhinovirus infections. Epidemiol. Rev. 10, 242–258.
Hers, J.F.P., Mulder, J., 1961. Broad aspects of the pathology and pathogenesis of human influenza. Am. Rev. Resp. Dis. 83, 84–89.
Hinds, W.C., 1982. Aerosol Technology. Wiley, New York.
Homeland Security Council, 2006. National Strategy for Pandemic Influenza: Implementation Plan. The White House, Washington.
International Commission on Radiological Protection (ICRP), 1994. ICRP Publication 66: Human respiratory tract model for radiological protection. Ann. ICRP 24, 36–54 and 231–299 (Pergamon Press, New York).

Jennings, L.C., Dick, E.C., 1987. Transmission and control of rhinovirus colds. Eur. J. Epidemiol. 3, 327–335.

Kaiser, L., Henry, D., Flack, N.P., Keene, O., Hayden, F.G., 2000. Short-term treatment with zanamivir to prevent influenza: results of a placebo-controlled study. Clin. Infect. Dis. 30, 587–589.

Karim, Y.G., Ijaz, M.K., Sattar, S.A., Johnson-Lussenburg, C.M., 1985. Effect of relative humidity on the airborne survival of rhinovirus-14. Can. J. Microbiol. 31, 1058–1061.

Khan, T.A., Higuchi, H., Marr, D.R., Glauser, M.N., 2004. Unsteady flow measurements of human microenvironment using time resolved particle image velocimetry. RoomVent 2004, Coimbra, Portugal, September 5–8, 2004.

Knight, V., 1973. Airborne transmission and pulmonary deposition of respiratory viruses. In: Knight, V. (Ed.), Viral and Mycoplasmal Infections of the Respiratory Tract, pp. 1–9. Lea & Febiger, Philadelphia.

Knight, V., Fedson, D., Baldini, J., Douglas, R.G. Jr., Couch, R.B., 1970. Amantadine therapy of epidemic influenza A_2 (Hong Kong). Infect. Immun. 1, 200–204.

Le, Q.M., Kiso, M., Someya, K., Sakai, Y.T., Nguyen, T.H., Nguyen, K.H.L., Pham, N.D., Ngyen, H.H., Yamada, S., Muramoto, Y., Horimoto, T., Takada, A., Goto, H., Suzuki, T., Suzuki, Y., Kawaoka, Y., 2005. Avian flu: isolation of drug-resistant H5N1 virus. Nature 437, 1108.

Leadbetter, M.R., Lindgren, G., Holger, R., 1980. Extremes and Related Properties of Random Sequences and Processes. Springer, New York.

Lloyd-Smith, J.O., Schreiber, S.J., Kopp, P.E., Getz, W.M., 2005. Superspreading and the impact of individual variation on disease emergence. Nature 438, 355–359.

Longini, I.M. Jr., Koopman, J.S., 1982. Household and community transmission parameters from final distributions of infections in households. Biometrics 38, 115–126.

Loosli, C.G., Lemon, H.M., Robertson, O.H., Appel, E., 1943. Experimental air-borne influenza infection. I. Influence of humidity on survival of virus in air. Proc. Soc. Exp. Biol. 53, 205–206.

Loudon, R.G., Brown, L.C., 1967. Cough frequency in patients with respiratory disease. Am. Rev. Resp. Dis. 96, 1137–1143.

Loudon, R.G., Roberts, R.M., 1967. Droplet expulsion from the respiratory tract. Am. Rev. Resp. Dis. 95, 435–442.

Markel, H., Stern, A.M., Navarro, J.A., Michalsen, J.R., 2006. A historical assessment of nonpharmaceutical disease containment strategies employed by selected U.S. communities during the second wave of the 1918–1920 influenza pandemic. Defense Threat Reduction Agency, Fort Belvoir, VA, http://www.dtra.mil/asco/DTRAFinalInfluenzaReport.pdf.

McLean, R.L., 1961. General discussion: the mechanism of spread of Asian influenza. Am. Rev. Respir. Dis. 83, 36–38.

Meschievitz, C.K., Schultz, S.B., Dick, E.C., 1984. A model for obtaining predictable natural transmission of rhinoviruses in human volunteers. J. Infect. Dis. 150, 195–201.

Miller, S.L., Nazaroff, W.W., 2001. Environmental tobacco smoke particles in multizone indoor environments. Atmos. Environ. 35, 2053–2067.

Morens, D.M., Rash, V.M., 1995. Lessons from a nursing home outbreak of influenza A. Infect. Control Hosp. Epidemiol. 16, 275–280.

Moser, M.R., Bender, T.R., Margolis, H.S., Noble, G.R., Kendal, A.P., Ritter, D.G., 1979. An outbreak of influenza aboard a commercial airliner. Am. J. Epidemiol. 110, 1–6.

Nicas, M., Sun, G., 2006. An integrated model of infection risk in a health-care environment. Risk Anal. 26, 1085–1096.

Nicas, M., Nazaroff, W.W., Hubbard, A., 2005. Toward understanding the risk of secondary airborne infection: emission of respirable pathogens. J. Occup. Environ. Hyg. 2, 143–154.

Niinimaa, V., Cole, P., Mintz, S., Shephard, R.J., 1980. The switching point from nasal to oronasal breathing. Respir. Physiol. 42, 61–71.

Papineni, R.S., Rosenthal, F.S., 1997. The size distribution of droplets in the exhaled breath of healthy subjects. J. Aer. Med. 10, 105–116.

Phelps, E.B., 1942. The state of suspension of bacteria in the air as measured by settling rates. In: Aerobiology, AAAS, Publication No. 17, pp. 133–137. Washington.

Rampey, A.H. Jr., Longini, I.M. Jr., Haber, M., Monto, A.S., 1992. A discrete-time model for the statistical analysis of infectious disease incidence data. Biometrics 48, 117–128.

Reed, S.E., 1975. An investigation of the possible transmission of rhinovirus colds through indirect contact. J. Hyg. (Camb.) 75, 249–258.

Rogers, G.N., D'Souza, B.L., 1989. Receptor binding properties of human and animal H1 influenza virus isolates. Virology 173, 317–322.
Rudnick, S.N., Milton, D.K., 2003. Risk of indoor airborne infection transmission estimated from carbon dioxide concentration. Indoor Air 13, 237–245.
Ryan, M.A.K., Christian, R.S., Wohlrabe, J., 2001. Handwashing and respiratory illness among young adults in military training. Am. J. Prev. Med. 21, 79–83.
Schaffer, F.L., Soergel, M.E., Straube, D.C., 1976. Survival of airborne influenza virus: effects of propogating host, relative humidity, and composition of spray fluids. Arch. Virol. 51, 263–273.
Sherman, M.H., Matson, N., 1997. Residential ventilation and energy characteristics. ASHRAE Trans. 103, 717–730.
Shinya, K., Ebina, M., Yamada, S., Ono, M., Kasai, N., Kawaoka, Y., 2006. Avian flu: influenza virus receptors in the human airway. Nature 440, 435–436.
Tannock, G.A., Gillett, S.M., Gillett, R.S., Barry, R.D., Hensley, M.J., Herd, R., Reid, A.L.A., Saunders, N.A., 1988. A study of intranasally administered interferon A (rIFN-alpha 2A) for the seasonal prophylaxis of natural viral infections of the upper respiratory tract in healthy volunteers. Epidem. Infect. 101, 611–621.
Tellier, R., 2006. Review of aerosol transmission of influenza A virus. Emerg. Infect. Dis. 12, 1657–1662.
Tumpey, T.M., Basler, C.F., Aguilar, P.V., Zeng, H., Solorzano, A., Swayne, D., Cox, N.J., Katz, J.M., Taubenberger, J.K., Palese, P., Garcia-Sastre, A., 2005. Characterization of the reconstructed 1918 Spanish influenza pandemic virus. Science 310, 77–80.
Wallace, L., 1996. Indoor particles: a review. Air Waste Manag. Assoc. 46, 98–126.
Wein, L.M., Atkinson, M.P., 2006. Assessing Infection Control Measures for Pandemic Influenza. Graduate School of Business, Stanford University, Stanford.
Wells, W.F., 1955. Airborne Contagion and Hygiene. Harvard University Press, Cambridge.
Winkler, K.C., 1973. In: Hers, J.F.P., Winkler, K.C. (Eds.), Aerosol Transmission and Airborne Infection. Wiley, New York.
Winther, B., Gwaltney, J.M. Jr., Mygind, N., Turner, R.B., Hendley, J.O., 1986. Sites of rhinovirus recovery after point inoculation of the upper airway. JAMA 256, 1763–1767.